Rodriguez, R., D. Jenkins, J.K. Leary and B.V. Mahnken. 2016. Herbicide Ballistic Technology: Spatial Tracking Analysis of Operations Characterizing Performance of Target Treatment. Trans ASABE. Transactions of the ASABE. 59(3): 803-809.

Rodriguez, R., D. Jenkins, J.K. Leary. 2015. Design and Validation of a GPS Logger System for Recording Aerial-Deployed Herbicide Ballistic Technology Operations. *IEEE Sensors. 15: 2078-2086.*

Leary, J.K., B. Mahnken, L. Cox, A. Radford, J. Yanagida, T. Penniman, D. Duffy and J. Gooding. 2014. Reducing Nascent Miconia (*Miconia calvescens* DC) Patches through Accelerated Interventions Utilizing Herbicide Ballistic Technology (HBT). Inv. Plant Sci. Mgmt. 7 (1) 164-175. DOI: 10.1614/IPSM-D-13-00059.1 ***Awarded 2015 Outstanding Paper for IPSM***

Leary, J.K., J. Gooding, J. Chapman, B. Mahnkan, A. Radford, L. Cox, 2013. Calibration of an Herbicide Ballistic Technology (HBT) Helicopter Platform Targeting Miconia (*Miconia calvescens* DC) in Hawaii. Inv. Plant Sci. Mgmt. 6(2) 292-303. DOI: 10.1614/IPSM-D-12-00026.1 (with press release; see popular media)

HERBICIDE BALLISTIC TECHNOLOGY: SPATIAL TRACKING ANALYSIS OF OPERATIONS CHARACTERIZING PERFORMANCE OF TARGET TREATMENT

R. Rodriguez III, J. J. K. Leary, D. M. Jenkins, B. V. Mahnken

ABSTRACT. *Since 2012, the Herbicide Ballistic Technology (HBT) platform has been deployed in helicopter operations with a mission to eliminate nascent populations of the invasive plant species miconia (*Miconia calvescens *DC), which is spreading across the East Maui Watershed in Hawaii. The HBT platform is a refined pesticide application system that pneumatically delivers encapsulated herbicide projectiles (i.e., paintballs) from a long range (up to ~30 m) and varying attitude. This onboard system provides accurate, effective treatment of individual plant targets occupying remote, inaccessible portions of the forested landscape. Statistics of operational performance are acquired through GIS analyses of recorded GPS data assigned to treated plant targets. Recently, we have developed a telemetry system for HBT applications (HBT-TS) to enhance the attribute data of target treatments. The HBT-TS integrates a hardware sensor with the electropneumatic marker that is actuated by the trigger to generate time-stamped, geo-referenced attribute data, including target assignment, azimuth, tilt, and range determined from the applicator position, for every projectile discharged. With target assignments, the HBT-TS records the estimated dose applied to each target. Furthermore, the time stamps show that the actual time to administer projectiles (i.e., target treatment) is a minor component of the total time on target. By tracking the orientation and distance of the discharged projectile, we can calculate a precise offset target location relative to the applicator position and provide a more accurate interpretation of the herbicide use rate (g acid equivalent ha^{-1}) based on the known amount of herbicide contained in each projectile and the final placement on the landscape. We acknowledge the challenges of GPS inaccuracies while recording in a dynamic environment (i.e., a moving platform in extreme topography), albeit with increased precision. Regardless, the current state of the HBT-TS technology enhances operational intelligence relevant to landscape-scale invasive species management.*

Keywords. *Aerial application, GIS, GPS,* Miconia calvescens *DC, Remote sensing, Telemetry.*

The Hawaiian archipelago is the most isolated group of islands on Earth, resulting in the evolution of endemic, highly specialized biotic communities (Carlquist, 1970; Mueller-Dombois et al., 1981; Stone and Scott, 1985). Currently, approximately 1100 endemic plant species and 4600 introduced exotic species have been catalogged, of which about 800 are considered invasive (Stone and Scott, 1985). These invasive plant incursions are threatening the ecological integrity and function of Hawaii's forested watersheds (Cox, 1999; Lindenmayer et al., 2000; Loope and Kraus, 2009; Loope et al., 2004; Mooney and Drake, 1986; Stone et al., 1992).

One of the most significant plant invasions in Hawaii is miconia (*Miconia calvescens* DC) in the East Maui Watershed (EMW). The EMW is 55,000 ha of forested landscape on the northeastern slope of Haleakala volcano. Miconia was introduced as an ornamental nursery stock plant in Hana in 1970. Today, the core infestation is approaching 1000 ha surrounding Hana, with small nascent populations spread across 20,000 ha of the EMW. Interventions on these incipient outlier populations are critical to maintaining an effective containment strategy for protecting the most intact endemic forest areas. The extreme topography and remote location of the EMW are major impediments to effective intervention with ground-based operations (Kueffer and Loope, 2009). Herbicide Ballistic Technology (HBT) is a novel pesticide application technology (registered as a 24(c) Special Local Need pesticide in Hawaii) that addresses these challenges with a capability to effectively treat individual plant targets with long-range accuracy and flexible attitude from a helicopter, while conducting surveillance operations (Leary et al., 2014).

Since 2012, HBT interventions have eliminated over 14,000 incipient miconia targets, as recorded by GPS from the applicator position on the aircraft. However, with an effective range of ~30 m, these coordinates are not the actual target locations. Furthermore, the herbicide dose has

Submitted for review in August 2015 as manuscript number ITSC 11474; approved for publication by the Information, Technology, Sensors, & Control Systems Community of ASABE in January 2016.

The authors are **Roberto Rodriguez III, ASABE Member,** Graduate Student, Department of Biosciences and Bioengineering, University of Hawaii at Manoa, Honolulu, Hawaii; **James J. K. Leary,** Extension Specialist, Department of Natural Resources and Environmental Management, University of Hawaii at Manoa, Kula, Hawaii; **Daniel M. Jenkins, ASABE Member,** Professor, Department of Biosciences and Bioengineering, University of Hawaii at Manoa, Honolulu, Hawaii; **Brooke V. Mahnken,** GIS Specialist, Maui Invasive Species Committee, Makawao, Hawaii. **Corresponding author:** Roberto Rodriguez III, 218 Agricultural Science Building, 1955 East-West Road, Honolulu, HI 96822; phone: 727-415-6712; e-mail: roberto6@hawaii.edu.

 © 2016 American Society of Agricultural and Biological Engineers ISSN 2151-0032 DOI 10.13031/trans.59.11474

been calculated as a composite average of the total estimated projectile inventory discharged to the total number of targets recorded. To enhance analyses of operations, a telemetry system was developed with sensor hardware integrated into the electro-pneumatic propulsion system (i.e., paintball marker) in which the data acquisition sequence is actuated by the trigger pull, populating a data matrix with the azimuth, tilt, target ID, time stamp, and geodetic coordinates for each projectile discharged (Rodriguez et al., 2015). In this article, we report on a second-phase iteration of the telemetry system for HBT applications (HBT-TS) with a laser range finder augmenting the sensor hardware, which introduces the capability to geometrically calculate the offset location of the target from the applicator position. This further increases the resolution of the calculated metrics pertinent to the operation, including spatial statistics using the distance to the target to estimate the final position of each projectile and the herbicide use rate.

In 2013, we developed our first iteration of a fully operational HBT-TS that could perform basic functions in recording geo-referenced locations with time stamps of all actions specific to an HBT operation (Rodriguez et al., 2015). The telemetry hardware consists of a printed circuit board populated with several sensors, including barometric altimeter, gyroscope, magnetic compass, and triple-axis accelerometer that transmit data via Bluetooth to a devoted software application written in Android open source code. We have since initiated phase II development of the HBT-TS with incorporation of a laser range finder (LRF) capable of quantifying the distance to target treatment (up to 40 m). As described by Rodriguez et al. (2015), the HBT-TS sensor device is mounted parallel to the barrel on the side picatinny rail, a series of extrusions with T-shaped cross-sections used to mount accessories onto a firearm or similar device, of the electro-pneumatic marker (BT TM7, Kee Action Sports LLC, Sewell, N.J.), with an interrupt-enabled I/O pin connected to the open-drain contact controlling the firing-solenoid current. When this signal is observed to go to ground (i.e., projectile is discharged), the system records the current time along with the most current sensor data attributed to the projectile and target (fig. 1).

Figure 1. HBT-TS mounted to electro-pneumatic marker with major parts labeled.

Materials and Methods

A total of five aerial miconia interventions were conducted in February and March of 2015 for testing the second-generation HBT-TS with LRF in a dynamic operational setting. The orientation sensors on the device were calibrated using a compass and clinometer (360PC/360R Suunto Tandem, Amer Sports Corp., Helsinki, Finland) prior to the first operation of each day. The barometric altimeter was calibrated before each operation using the known elevation of the heliport or landing zone. All operations were conducted using a Hughes 500D helicopter with the applicator positioned port side behind the pilot, so the pilot and applicator shared the field of view for target detection and engagement. Upon detection, the applicator pressed the target acquisition button (fig. 1), establishing a unique target ID to be assigned to all subsequent projectiles discharged until the next acquisition. In the meantime, the pilot approached the target for a clear line of sight within effective range and held the position while the applicator administered the projectile dose to the target. In these operations, all projectiles (x = 6845) were correctly assigned to targets (n = 365).

The distribution of the applicator GPS position and calculated offset coordinates for each target were calculated using the circular map accuracy standard (CMAS) and spherical accuracy standard (SAS). The CMAS is the magnitude of the radius of the smallest circle, in the plane tangent to the Earth at the mean location corresponding to latitude and longitude, containing 90% of the recorded positions (USBB, 1947). The SAS is the magnitude of the radius of the smallest sphere containing 90% of the recorded positions (Greenwalt, 1962). Assuming normally distributed errors in the horizontal coordinates, CMAS can be described mathematically as:

$$\mathrm{CMAS} = 2.1460\sigma_c \tag{1}$$

where σ_c is the circular standard error, which can be approximated by:

$$\sigma_c \approx \frac{1}{2}\left(\sigma_x + \sigma_y\right) \tag{2}$$

where σ_x and σ_y are the standard deviations in horizontal position corresponding to errors in latitude and longitude, respectively, assuming that the larger of the two is less than five times the magnitude of the other (Greenwalt, 1962). SAS can be estimated as:

$$\mathrm{SAS} = 2.5\sigma_s \tag{3}$$

where σ_s is the spherical standard error approximated by:

$$\sigma_s \approx \frac{1}{3}\left(\sigma_x + \sigma_y + \sigma_z\right) \tag{4}$$

where σ_z is the standard deviation in altitude, assuming that

the smallest of the three component standard deviations is not less than 0.35 times the magnitude of the largest (Greenwalt, 1962).

The interquartile ranges of the spatial statistics are presented along with the standard deviations, which are composed of deliberate adjustments (e.g., offsets due to aiming the marker at different parts of the target to disperse herbicide) in addition to some small random variation in sensor response. Since the azimuth (θ) is capable of spanning the full 360°, the directional mean and standard deviation are calculated from equations 5 through 8 (Berens, 2009):

$$\bar{s} = \sum_{i=0}^{n} \sin\theta_i \tag{5}$$

$$\bar{c} = \sum_{i=0}^{n} \cos\theta_i \tag{6}$$

$$\bar{\theta} = \begin{cases} \arctan\left(\frac{\bar{s}}{\bar{c}}\right) & \bar{s} > 0,\ \bar{c} > 0 \\ \arctan\left(\frac{\bar{s}}{\bar{c}}\right) + 180^\circ & \bar{c} < 0 \\ \arctan\left(\frac{\bar{s}}{\bar{c}}\right) + 360^\circ & \bar{s} < 0,\ \bar{c} > 0 \end{cases} \tag{7}$$

$$s_\theta = \sqrt{-2\ln\left(\bar{s}^2 + \bar{c}^2\right)} \tag{8}$$

Herbicide use rate (HUR) is the amount of pesticide applied per unit area, e.g., g acid equivalent (ae) ha^{-1}. An HBT projectile contains 0.1994 g ae of the active ingredient triclopyr (HBT-G4U200, Nelson Paint Co., Kingsford, Mich.) and is estimated to produce a circular spatter pattern that has a radius of ~1 m (i.e., 3.14 m^2). Spatial analyses were performed to calculate the area of the footprint and HUR using ArcMap 10.1 (ESRI, Redlands, Cal.). Area footprints were calculated for each projectile, target, and total net treated area using the Buffer Analyses tool with 1 m radius and the Dissolve Type parameter set to None, List (using the identifier "Target_ID"), and All commands, respectively. To determine the HUR distribution across the entire treated area, a point density analysis was performed with a 0.0625 m^2 cell size and a 1 m circular neighborhood to measure the magnitude of the herbicide dose (0.1994 g ae projectile^{-1}; x = 6845) overlaid onto the total net area footprint created by the offset placement of the projectiles. Aspect values were extracted from a 10 m digital elevation model layer of Maui (NOAA, 2007) at each of the offset point coordinates to calculate the angular line of sight (L) to target with respect to the terrain aspect (m_A):

$$L = \theta - m_A \tag{9}$$

Results and Discussion

An HBT application is an advancement of a surveillance operation with the capability of immediate intervention on high-value, incipient plant targets. One of the critical attributes of HBT is the capability to efficiently and effectively treat targets occupying extreme terrain that are otherwise inaccessible (fig. 2). This includes situations where the applicator can engage a target from different lines of sight (fig. 2b) or multiple targets from a single applicator position with different trajectories (fig. 2c). Target engagement (upon detection) is a systematic process that momentarily deviates from the normal search pattern to approach and treat the target. Consistency in these treatment actions includes a steady position of the applicator, the attitude of the projectile, range to target, and treatment dose (table 1). Most of these statistics were slightly leptokurtic with a strong peak at the median, along with a minority of values as large, positive outliers, making the averages of most distributions somewhat larger than the corresponding medians.

The target dose had a median value of 15 projectiles with an interquartile range from 9 to 23 projectiles. This is less than the median of an average 24-projectile dose over the last three years of operations but is consistent with

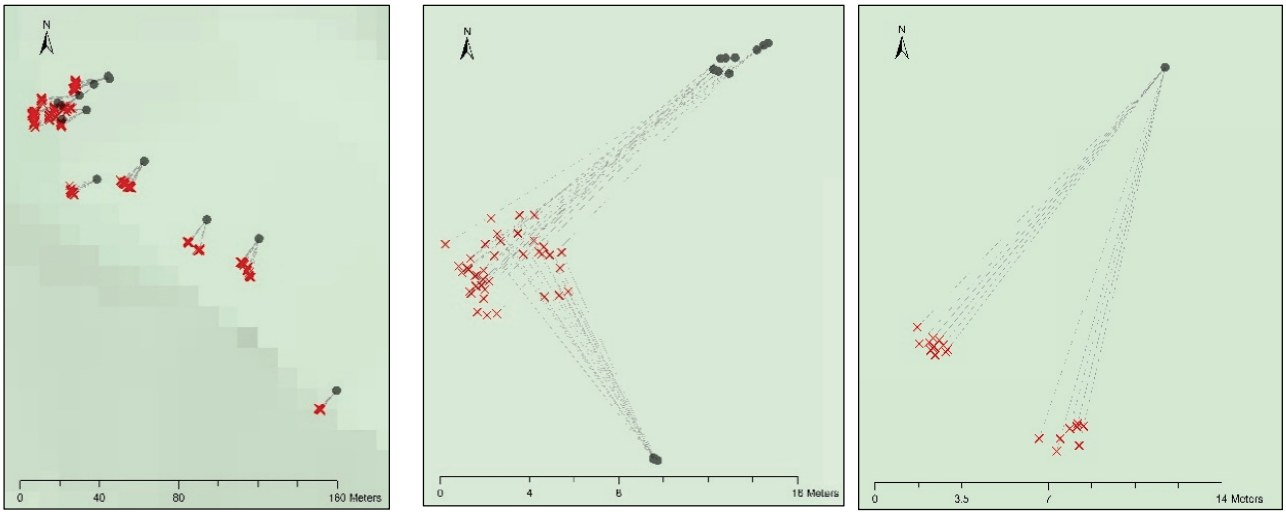

(a) (b) (c)

Figure 2. (a) Applicator (•) and target offset (×) locations calculated from range, azimuth, and tilt values (gray lines) overlaid on 10 m digital elevation model, (b) a target treated from multiple applicator positions, and (c) multiple targets treated from a single applicator position.

Table 1. Statistical analysis of HBT application. Range and tilt data are from entire population of projectiles (x = 6845). All other data, including those preceded by SD (standard deviation of the parameter), are for projectiles grouped by target (n = 365). Because azimuth to target is semi-random for each target, only the standard deviation of the projectile azimuth for each target is reported for these data.

Metric	Median	Interquartile Range	Average
Applicator precision and spatial statistics			
$CMAS_A$ (m)	0.7	0.1 to 1.5	1.1
SAS_A (m)	1.0	0.5 to 1.7	1.3
Range (m)[a]	15.2	13.3 to 17.8	15.6
SD range (m)	0.8	0.3 to 1.5	1.0
Tilt (°)[b]	-33.0	-43.4 to -23.1	-33.1
SD tilt (°)	1.0	0.7 to 1.5	1.3
SD azimuth (°)[c]	3.9	2.8 to 5.5	4.9
Target offset precision			
$CMAS_T$ (m)	1.7	1.1 to 2.3	1.9
SAS_T (m)	1.9	1.3 to 2.8	2.3
Treatment statistics			
Projectile dose[d]	15	9 to 23	18.7
HUR (g ae ha^{-1})[e]	2103.0	1628.5 to 2920.5	2459.7

[a] Distance to target measured by laser rangefinder.
[b] Tilt measured with respect to the horizontal plane.
[c] Azimuth measured with respect to geographic north.
[d] Number of projectiles discharged during target treatment.
[e] Herbicide use rate, with 0.1994 g ae per projectile and herbicide distribution area calculated from a 1 m radius created on target impact.

smaller targets becoming more common as more mature plants are eliminated (data not shown). The marker is a rapid fire, semi-automatic system with discharge rates of ~2.2 projectiles s^{-1} (fig. 3). Hence, the median treatment time is <7 s (data not shown). We suggest that the low CMAS and SAS precision values of the applicator position are predicated on this brief time period, while the helicopter is holding hover (table 1). The accuracy of the target locations is unknown, as the inaccessibility of the terrain makes ground truthing impossible. However, previous static experiments indicated that the position accuracy is comparable to that of other commercial-grade GPS units, with GPS error being the limiting factor (Rodriguez, 2015).

The CMAS and SAS values for the target offset location are less precise than the applicator position, where the deviations of the projectile's range and attitude (e.g., tilt and azimuth) had a compounding effect (table 1). These variations in the recorded attitude are primarily due to operator adjustment to cover and/or zero in on the target and account for 78% of the observed spread in estimated target offset locations in CMAS and 70% of the observed spread in SAS after accounting for random errors estimated from static measurements. The CMAS and SAS of the target offset locations show weak dependence on herbicide dose, and the SAS is not substantially larger than the CMAS (fig. 4). When a 1st/1st degree rational polynomial is fitted to the CMAS, the resulting horizontal asymptote is 5.0 m. This equates to a maximum treatment diameter of 10 m, consistent with the diameter of miconia (Harling et al., 1973), and a maximum treatment area of approximately 80 m^2. The same process for SAS shows a similar asymptote at 6.2 m, equating to a treatment volume of approximately 560 m^3. If the treatment area is instead considered an annular region comprising of 90% of the deviation observed in the azimuth and range, then the total area calculated is 12.5 m^2. Similarly, considering the volume bounded by 90% of the deviation seen in the azimuth, tilt, and range, the total volume would be 9.4 m^3. Adding the CMAS and SAS to these values results in an average treatment area of 16.0 m^2 and treatment volume of 19.1 m^3 per treated plant. This estimate of the treatment area more closely resembles that calculated by GIS analysis and better reflects the actual shape of the treatment area (fig. 6b).

These aerial operations were conducted by searching for miconia occupying extreme terrain (e.g., slopes up to 70°). Operational flight lines are typically transects running parallel to the contour, with a bias on the port side where the pilot and applicator share the same field of view, i.e., ~ 270° to 330° relative to the aircraft bearing, offering direct observation by both parties of the terrain search area. When a target was detected, the pilot approached the target to a median distance of 15.2 m with an interquartile range not exceeding 20 m and always approached from above the target where the median tilt of the applicator was -33° with respect to the horizontal plane and with an interquartile range less than -20° (table 1). From these positions, targets were confronted with lines of sight almost directly opposite

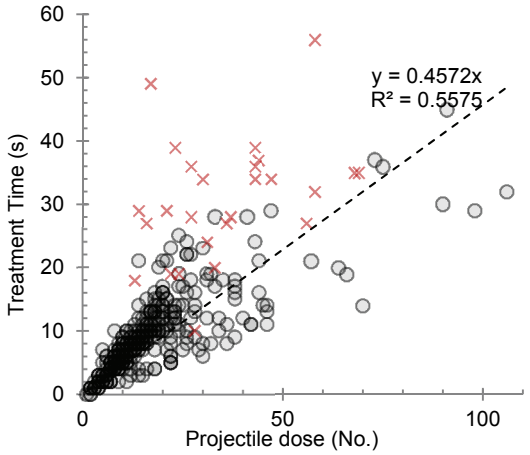

Figure 3. Treatment time dependence on projectile dose (○; n = 338; y = 0.4572x; R^2 = 0.5575). Targets requiring reload and/or applicator repositioning (×) result in larger treatment time (outliers; n = 27).

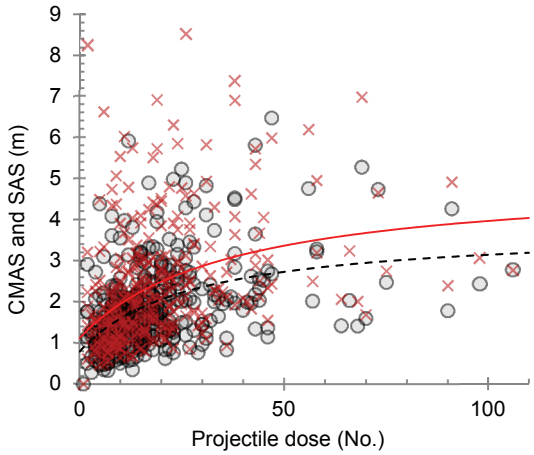

Figure 4. CMAS (○) and SAS (×) of predicted target offset locations versus projectile dose (n = 365; CMAS R^2 = 0.19; SAS R^2 = 0.15). Dashed line indicates CMAS trend, and solid line indicates SAS trend.

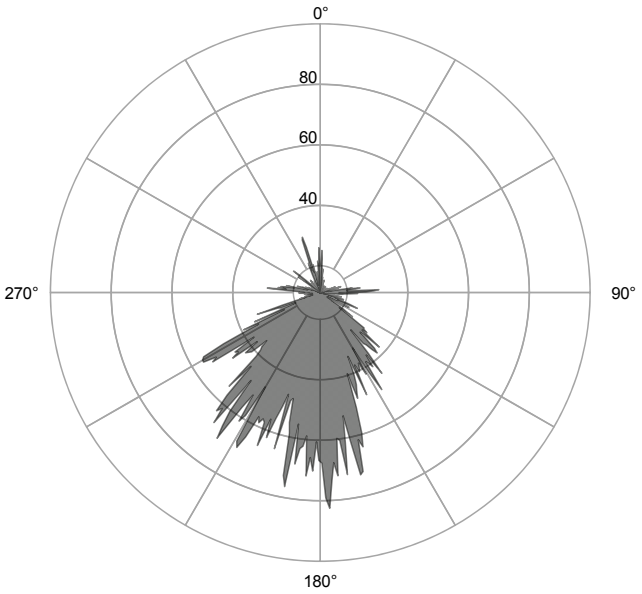

Figure 5. Frequency plot of projectile azimuth with respect to the terrain aspect at the predicted target location (x = 6845).

the terrain aspect with a median azimuth of 191° (fig. 5). The terrain aspect is the vector normal to the terrain surface projected into the horizontal plane and is also assumed to be the aspect for the plant colonizer such that an angle of 180° in the plot indicates application directly into the contour of the hillside (i.e., plant target). The interquartile range was 163° to 222°, where angles >180° could indicate efficiency in approaching the target immediately upon detection, while angles <180° might relate to efforts to reposition the aircraft for a better line of sight, free of obstacles (e.g., tree canopy). Angles measured beyond perpendicular (i.e., >270° and <90°) are improbable and most likely represent the compounding errors associated with the GPS and the terrain model, particularly along ridges where aspect can change dramatically with position.

Time on target (ToT) is the total time spent in the target acquisition and treatment process. In a previous study, Leary et al. (2014) found total search effort to be dependent on target density, where the slope value was equivalent to the added time for every target encountered (i.e., ToT). The actual treatment time recorded as the time interval between the first and last projectile discharged was a minor time element in these operations (table 2). The majority of the time appears to have been spent approaching and maneuvering the applicator into position for target treatment. Time spent reloading projectiles (19.1 ±8.3 s) and repositioning the applicator (20.1 ±10.8 s) were other time elements contributing to ToT, although these activities were

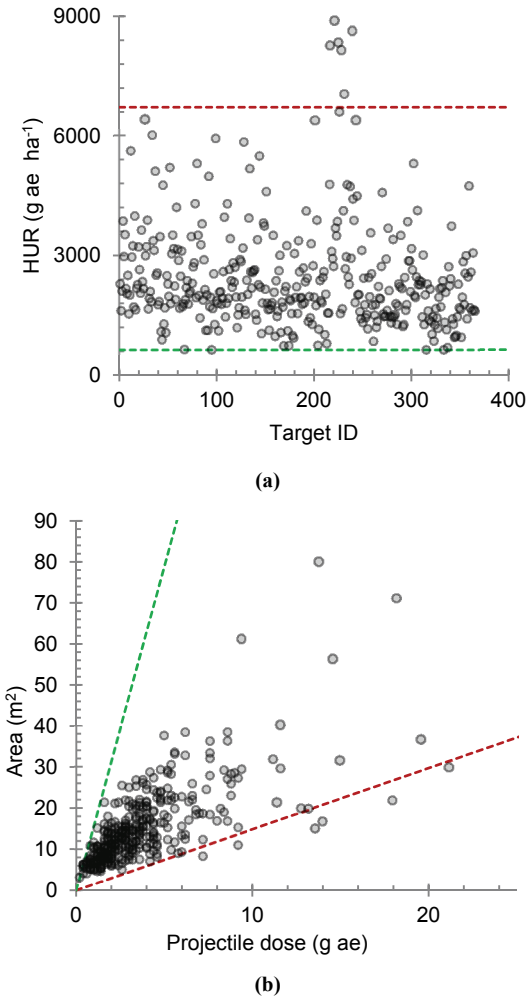

Figure 6. (a) Target herbicide use rate (HUR; g ae ha^{-1}; n = 365; x = 6845) calculated from the projectile dose and net area of the projectile offset locations buffered with a 1 m radius, and (b) net target offset area created by projectile dose. Green dashed line is the HUR for a single isolated projectile, and red dashed line is the maximum allowable HUR according to the registered pesticide label.

not required for the majority of targets treated.

A single projectile creates a treatment footprint area estimated at 3.14 m^2 with an equivalent HUR of 634.7 g ae ha^{-1}, which is 9.4% of the maximum allowable rate (i.e., 6,720 g ae ha^{-1} year^{-1}). The mean target HUR in these operations was 2,460 g ae ha^{-1}, with 98.3% of targets below the maximum HUR (fig. 6a). The average target dose and area footprint were 3.6 g ae and 15.1 m^2 for targets below the maximum HUR (fig. 6b). On the other hand, for those six targets that exceeded the maximum HUR, the average area footprint was only slightly higher at 17.2 m^2, while the average dose increased to 13.8 g ae. These high doses are

Table 2. Time elements of the target acquisition and treatment process.

Name[a]	Activity	Characteristic	Time (s)
Time on target	Time spent at a target not in active search	Total time	55.5 ±4.9
Treatment time	Time to administer projectile dose to target	Time between first and last projectile discharged	9.2 ±6.5
Reload time	Reloading hopper with projectiles, interrupting treatment action	Reload every ~160 projectiles	19.1 ±8.3
Reposition time	Relocating to treat target from a different location	Standard deviation of azimuth and range of target increase substantially	20.1 ±10.8

[a] Time on target was extrapolated from the slope of search effort dependent on target densities encountered, as described by Leary et al. (2014). Treatment time (n = 338), reload time (n = 20), and reposition time (n = 7) were direct empirical values derived from the time stamps.

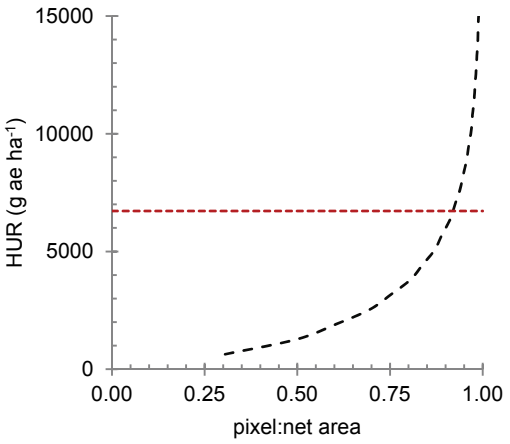

Figure 7. Cumulative distribution plot of pixel-scale (0.0625 m^2) HUR for the entire area treated in this study. Red dashed line is the maximum allowable HUR.

likely artifacts of treating larger (mature) targets or due to inaccuracies in treating smaller targets. The total area footprint of these excessive targets was 103 m^2, or 1.9% of the total target area. The total net area footprint was 4,938 m^2, which was saturated 435.5% by the gross projectile footprint area (i.e., 3.1416 m^2 × 6845 projectiles), with a net HUR that was 41.1% of the maximum allowable rate. In this case, 6.1% of the total pixel area (i.e., 371.1 m^2) exceeded the maximum HUR (fig. 7) but was heterogeneously scattered at a sub-meter scale. The analyses of HBT-TS data highlight the fine-scale presentation of herbicide application and the opportunity for high-resolution analyses.

CONCLUSION

The HBT platform is a precision pesticide application system customized for incipient species control where operational performance has both spatial and temporal relevance. The second-phase HBT-TS with LRF has substantially enhanced the resolution of this data-driven process with the capability to (1) accurately measure treatment time, (2) better interpret applicator position and approach to target, (3) geometrically calculate target offset location, and (4) determine HUR with high resolution. While precision is a highlight of the HBT-TS, accuracy remains a challenge for all technologies that rely on GPS in a dynamic environment. Future work is proposed to investigate the transition of this technology proven in manned aerial systems toward adoption in unmanned aerial systems.

ACKNOWLEDGEMENTS

This project was funded in parts by the USDA Forest Service Special Technology Development Program (Award R5-2012-01) through collaboration with the Hawaii Department of Land and Natural Resources Forest Health Program, the Hawaii Invasive Species Council, the USDA Hatch Act Formula Grant Project 112H, and the Maui County Office of Economic Development and Department of Water Supply.

REFERENCES

Berens, P. (2009). CircStat: A MATLAB toolbox for circular statistics. *J. Stat. Software, 31*(10). http://dx.doi.org/10.18637/jss.v031.i10

Carlquist, S. J. (1970). *Hawaii: A Natural History: Geology, Climate, Native Flora and Fauna above the Shoreline.* Garden City, N.Y.: American Museum of Natural History.

Cox, G. W. (1999). *Alien Species in North America and Hawaii*. (1st ed.). Washington, D.C.: Island Press.

Greenwalt, C. R. (1962). *Principles of Error Theory and Cartographic Applications*. ACIC Technical Report 96. St. Louis, Mo.: Aeronautical Chart and Information Center.

Harling, G., Sparre, B., Andersson, L., & Persson, C. (1973). *Flora of Ecuador.* Gothenborg, Sweden: University of Gothenborg, Department of Systematic Botany.

Kueffer, C., & Loope, L. L. (2009). Prevention, early detection, and containment of invasive, nonnative plants in the Hawaiian Islands: Current efforts and needs. Honolulu, Hawaii: University of Hawaii at Manoa, Department of Botany, Pacific Cooperative Studies Unit.

Leary, J. J., Mahnken, B. V., Cox, L. J., Radford, A., Yanagida, J., Penniman, T., ..., Gooding, J. (2014). Reducing nascent miconia (*Miconia calvescens*) patches with an accelerated intervention strategy utilizing herbicide ballistic technology. *Invasive Plant Sci. Mgmt., 7*(1), 164-175. http://dx.doi.org/10.1614/IPSM-D-13-00059.1

Lindenmayer, D. B., Margules, C. R., & Botkin, D. B. (2000). Indicators of biodiversity for ecologically sustainable forest management. *Conserv. Biol., 14*(4), 941-950. http://dx.doi.org/10.1046/j.1523-1739.2000.98533.x

Loope, L., & Kraus, F. (2009). Preventing establishment and spread of invasive species: Current status and needs. In *Conservation of Hawaiian Forest Birds: Implications for Island Birds.* New Haven, Conn.: Yale University Press.

Loope, L., Starr, F., & Starr, K. I. (2004). Protecting endangered plant species from displacement by invasive plants on Maui, Hawaii. *Weed Tech., 18*(1), 1472-1474. http://dx.doi.org/10.1614/0890-037X(2004)018[1472:PEPSFD]2.0.CO;2

Mooney, H. A., & Drake, J. A. (Eds.). (1986). *Ecology of Biological Invasions of North America and Hawaii*. Ecological Studies Vol. 58. New York, N.Y.: Springer-Verlag. http://dx.doi.org/10.1007/978-1-4612-4988-7

Mueller-Dombois, D., Bridges, K. W., & Carson, H. L. (Eds.). (1981). *Island Ecosystems: Biological Organization In Selected Hawaiian Communities.* Stroudsburg, Pa.: Hutchinson Ross.

NOAA. (2007). Digital elevation models (DEMs) for the main eight Hawaiian Islands. Washington, D.C.: National Oceanic and Atmospheric Administration. Retrieved from https://data.noaa.gov/dataset/digital-elevation-models-dems-for-the-main-8-hawaiian-islands

Rodriguez, R. (2015). A custom GPS recording system for improving operational performance of aerially deployed herbicide ballistic technology. MS thesis. Honolulu, Hawaii: University of Hawaii at Manoa.

Rodriguez, R., Jenkins, D. M., & Leary, J. J. (2015). Design and validation of a GPS logger system for recording aerially deployed herbicide ballistic technology operations. *IEEE Sensors J., 15*(4), 2078-2086. http://dx.doi.org/10.1109/JSEN.2014.2371896

Stone, C., & Scott, J. M. (1985). *Hawaii's Terrestrial Ecosystems: Preservation and Management.* Honolulu, Hawaii: University of Hawaii: Cooperative National Park Resources Studies Unit.

Stone, C., & Smith, C., & Tunison, J. T. (Eds.). (1992). *Alien Plant Invasions in Native Ecosystems of Hawaii: Management and Research.* Honolulu, Hawaii: University of Hawaii Press.

USBB. (1947). *United States National Map Accuracy Standards*. Washington, D.C.: U.S. Bureau of the Budget.

NOMENCLATURE

CMAS = circular mapping accuracy standard
EMW = East Maui Watershed
HBT = Herbicide Ballistic Technology
HBT-TS = HBT telemetry system
HUR = herbicide use rate
LRF = laser rangefinder
SAS = spherical accuracy standard
SD = standard deviation (for a single target)
ToT = time on target

Design and Validation of a GPS Logger System for Recording Aerially Deployed Herbicide Ballistic Technology Operations

Roberto Rodriguez, III, *Student Member, IEEE*, Daniel M. Jenkins, and James J. K. Leary

***Abstract*— Herbicide ballistic technology (HBT) is an electro-pneumatic delivery system designed for administering 17.3-mm herbicide-filled projectiles (e.g., paintballs) to visually acquired weed targets. Currently, HBT is being deployed from a Hughes 500D helicopter platform in aerial surveillance operations to eliminate satellite invasive weed populations in remote natural watershed areas of Maui (HI, USA). In an effort to improve operations, we have integrated GPS and other sensor hardware into the electropneumatic device for instantaneous recording of time, origin, and trajectory of each projectile discharged by the applicator. These data are transmitted wirelessly to a custom android application that displays target information in real time both textually and graphically on a map.**

***Index Terms*— Data acquisition, geospatial analysis, global positioning system, sensor integration and fusion.**

I. Introduction

INVASIVE, exotic plant species are threatening the endemic biological integrity of the Hawaiian archipelago [1]–[7]. Moreover, the islands' extreme topography and dense vegetation are an impediment to effective mitigation [8]. Herbicide Ballistic Technology (HBT) is a concept to address these challenges with a novel capability to treat invasive plant targets with long-range accuracy [9]. In previous implementations, the HBT platform enhances helicopter surveillance operations with the capability of eliminating high-risk satellite populations of invasive plant targets, which are occupying remote inaccessible areas of watershed [10].

II. Background

The HBT platform is an herbicide delivery system currently registered in the state of Hawaii as a Special Local Need pesticide for treating nascent miconia (*Miconia calvescens* DC) and strawberry guava (*Psidium cattleianum*) patches in remote natural areas [9]. The basic concept of HBT is the encapsulation of an active herbicide formulation into 17.3 mm soft-gel projectiles (i.e., paintballs) for accurate, long-range delivery to weed target via propulsion from an electro-pneumatic marker. Projectiles can be delivered to a target with an estimated effective range of ∼30m, presenting novel opportunities for managing areas with extreme, inaccessible landscapes (e.g., ravines and cliff faces).

The adoption of satellite navigation (utilizing GPS and GLONASS) in HBT operations has allowed for the acquisition of large data sets leading to explicit spatial and temporal performance evaluation of an operation [10]. Current op erational procedures call for reference points to be recorded for each target treated using a consumer-grade GPS receiver capturing latitude, longitude, elevation and timestamp. At the end of each operation, the applicator also records the estimated total consumption of projectiles that is later translated into the average dose rate for the total targets treated in that operation.

Attitude and heading reference systems (AHRS) provide the roll, pitch and yaw of a body and are commonly used for navigation purposes. Recent development in micro-electro-mechanical systems (MEMS) based AHRS systems are being used in a number of applications, including unmanned aerial vehicles (UAV) [11], commercial airplanes [12], along with terrestrial [13] and submerged navigation [14]. However, many of these systems have a large profile and require wired connections to data recording devices making them ill suited for implementation with the HBT platform.

To enhance operational data acquisition, a custom, prototype HBT-Logging System (HBT-LS) was developed for integration with the electro-pneumatic marker automating data acquisition for every projectile discharged. Data acquired includes the above mentioned spatial and temporal assignments, along with added attributes for tilt and azimuth of the marker position (Fig. 1). New analyses of HBT-LS data sets include: (i) accurate accounts of projectile dose rates assigned to each target, (ii) the time to deliver projectile dose to target and (iii) offset projections of the actual target location.

Here in, we report on the basic hardware and software specifications of HBT-LS with static and dynamic calibrations in controlled and operational settings, respectively. This includes a discussion on improvements in the data management process and technology limitations requiring further development.

Manuscript received September 15, 2014; revised November 3, 2014; accepted November 11, 2014. Date of publication November 20, 2014; date of current version January 29, 2015. This work was supported in part by the U.S. Department of Agriculture (USDA) Forest Service, in part by the Special Technology Development Program under Award R5-2012-01 through the Hawaii Department of Land and Natural Resources Forest Health Program, in part by the Hawaii Invasive Species Council under Award POC 40466, in part by the USDA Hatch Act Formula Grant under Project 112H, and in part by the USDA Renewable Resources Extension Act. The associate editor coordinating the review of this paper and approving it for publication was Prof. Octavian Postolache.

R. Rodriguez III and D. M. Jenkins are with the Department of Molecular Bioscience and Biological Engineering, University of Hawaii at Manoa, Honolulu, HI 96822 USA (e-mail: roberto6@hawaii.edu; danielje@hawaii.edu).

J. J. K. Leary is with the Department of Natural Resources and Environmental Management, University of Hawaii at Manoa, Honolulu, HI 96822 USA (e-mail: leary@hawaii.edu).

Color versions of one or more of the figures in this letter are available online at http://ieeexplore.ieee.org.

Digital Object Identifier 10.1109/JSEN.2014.2371896

1530-437X © 2014 IEEE. Personal use is permitted, but republication/redistribution requires IEEE permission.
See http://www.ieee.org/publications_standards/publications/rights/index.html for more information.

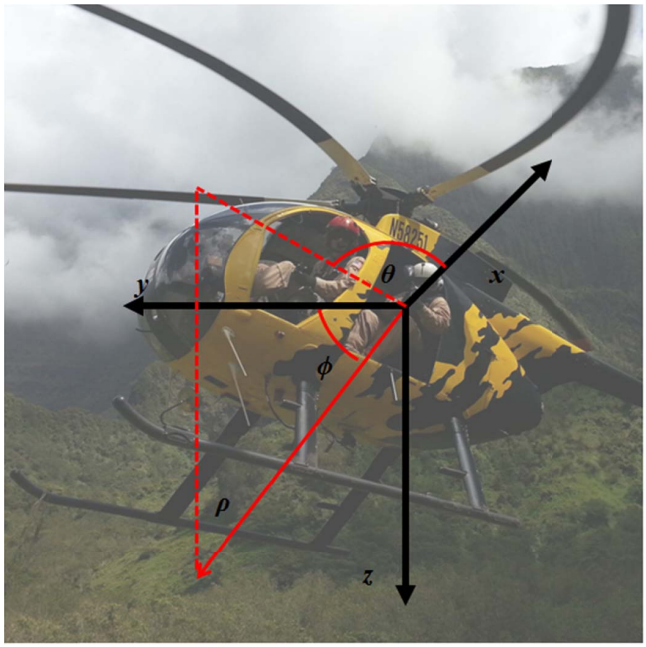

Fig. 1. Spherical coordinate system to describe plant target locations with applicator as the origin.

III. Sensor Development

A. Hardware Design

The relevant data to be recorded include the position (latitude, longitude, and altitude), azimuth and tilt of the marker, depicted in Fig. 1, as well as each discharge of a projectile and the unique target IDs and descriptions of each targeted plant. Latitude and longitude are recorded within a custom Android user interface from the built in GPS chip (Broadcom BCM4751) on the interfacing Android device. Most non-GPS information is recorded on a custom circuit (Fig. 2) with individual sensors communicating to a simple 8-bit microcontroller (ATMEGA328P-MUR, Atmel Corp., San Jose, CA) which transmits data wirelessly to the Android application through a serial Bluetooth module (RN42, Roving Networks, Los Gatos, CA). Altitude is estimated from barometric pressure measurements based on empirical relationships (MPL3115A2, Freescale Semiconductor, Austin TX). Azimuth and tilt are recorded from inertial (MPU-6050, InvenSense, San Jose, CA) and magnetic (LSM303DLHTR, STMicroelectronics, Geneva, Switzerland) sensors as described below. Projectile discharge is identified by an interrupt triggered by the transistor sinking the solenoid current in the marker, and similarly a momentary contact switch triggers an interrupt to indicate acquisition of a new target (for which a new target ID is automatically assigned). Descriptive information for each target is coded by user selection of radio buttons in the Android interface. In our case, descriptions are coded for the developmental stage of the plant with options for "Juvenile" (not yet bearing fruits/seeds), "Mature" (flower/fruit bearing), or "Survivor" (showing sub-lethal symptoms resulting from a previous herbicide application). Description reverts to the default "Juvenile" for each newly engaged target, as these are by far the most commonly encountered plants in our operations to eliminate incipient satellite populations.

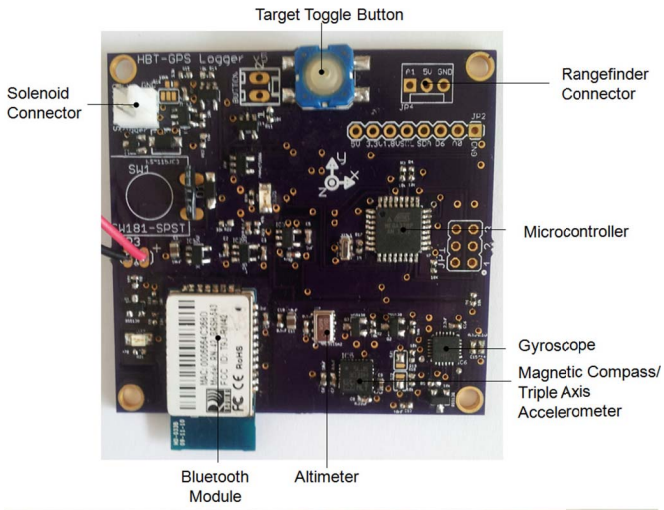

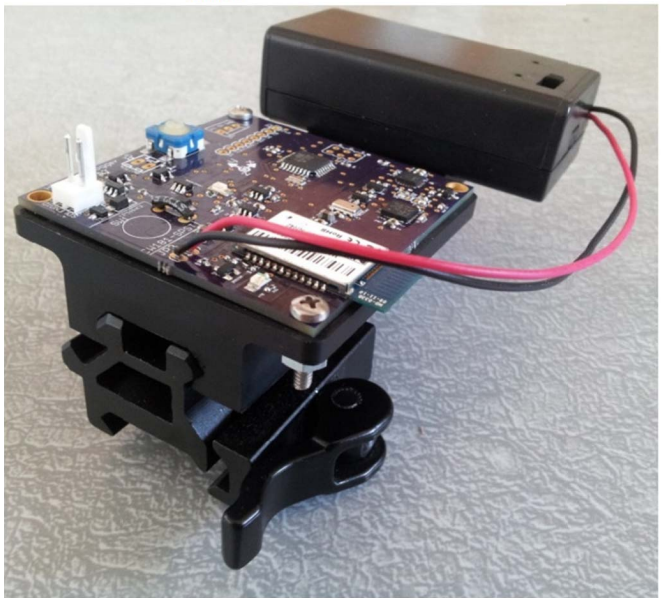

Fig. 2. HBT-Logger System (HBT-LS) with annotations for major components (top), and mounted on rail attachment system (bottom).

1) Altitude: Altitude is automatically inferred from observed barometric pressure (MPL3115A2, Freescale Semiconductor) based on the following internal empirical relationship, by setting the "ALT" bit on Control Register 1 of the sensor:

$$h = 44330.77\left[1 - \left(\frac{p}{p_0}\right)^{0.1902632}\right] + h_{\text{off}} \qquad (1)$$

where h is the height (in meters), p is the pressure (in Pascals), p_0 is the sea level pressure, and h_{off} is the offset in the determined height. To calibrate for variations in barometric pressure, sensors are calibrated at the start of each operation based on the known elevation at the landing site. This known elevation is used by the calibration activity of the Android device to estimate the current sea level pressure based on the current barometric pressure and its empirical relationship with altitude. The new estimate of sea level pressure reference is communicated to the microcontroller and loaded into the "Barometric Pressure Input" Registers of the MPL3115A2.

2) Azimuth and Tilt: The azimuth and tilt, represented by θ and φ in a spherical coordinate system (Fig. 1), are recorded using a triple axis gyroscope/accelerometer (MPU-6050) and a triple-axis tilt-compensated magnetic compass (LSM303DLHTR). Redundant measurements of orientation were made from these devices to facilitate identification and compensation for drift in the azimuth estimated from the gyroscope, or deviations in compass readings resulting from local disturbances in geomagnetic field or interferences by magnetic fields originating from or shielded by the aircraft.

The calibration activity of the Android interface allows the user to overwrite the digitized values stored in device EEPROM corresponding to the maximum and minimum magnetic fields applied in each axis of the compass chip (which vary significantly between devices). This allows the measurements in each axis to be scaled to internally consistent measures of the field strength. This calibration requires the user to align each of 6 reference orientations ($+x$, $-x$, $+y$, $-y$, $+z$, $-z$) of the sensor coordinates with the peak geomagnetic field at the given location. As a result, the 3-D vector of any arbitrary magnetic field is estimated accurately with respect to the marker coordinate system, and vector operations are implemented by the microcontroller to project this vector onto a horizontal plane compensated for tilt and roll of the marker estimated from acceleration measurements on the same chip. These measurements provide an estimate of the orientation of the marker in the horizontal plane with respect to magnetic north. Marker orientation is estimated from the gyroscope readings using custom coded quaternion algebra on the quaternion output retrieved from the digital motion processor of the device using the manufacturer's software library (MotionAppsTM 5.0). The quaternion codes for the current orientation of the sensor with respect to the initial orientation at the startup of the sensor.

Magnetic declination is determined at the start of each operation by orienting the marker along a path aligned with true north (or any other given reference orientation) and communicating this reference orientation to the microcontroller so that the reference with respect to magnetic north can be recorded in EEPROM. On device startup (or recalibration), the marker orientation estimated by the gyroscope, projected onto the horizontal plane, is initialized to the current geographical orientation based on the tilt compensated compass reading corrected for magnetic declination. The marker position (latitude, longitude and altitude), azimuth, and tilt, as depicted in Fig. 1, can be used to infer target position based on overlaying projectile orientation and trajectories onto digital elevation maps, and/or using an estimated range to target, represented by ρ.

3) Trigger Detection: The electro-pneumatic marker discharges projectiles via an actuating solenoid. Projectile discharge is registered by an interrupt caused by a falling edge of this signal, using a custom implemented Schmitt Trigger to prevent multiple interrupts from a single transition and to shift the signal to the microcontroller logic level. The trigger signal is buffered by a voltage follower to prevent loading of the solenoid. In order to prevent triggering from artifacts of resonance in the inductive load associated with the same trigger pull, a latent period is enforced in software during which subsequent falling edges are not registered. This latent period is greater than the period for which oscillations associated with a single projectile discharge occur, but is smaller than the period at which projectiles can be discharged in rapid fire (i.e., >10 projectiles sec^{-1}).

B. Software Design

1) Calculating Plant Target Coordinates: The equations of motion for a spherical projectile travelling in air is [15]

$$m\ddot{\mathbf{r}} = m\dot{\mathbf{v}} = -\frac{1}{2}\rho_A A C_D \left|\vec{\mathbf{v}} - \vec{\mathbf{W}}\right|\left(\vec{\mathbf{v}} - \vec{\mathbf{W}}\right) + \frac{1}{2}\rho_A A C_L \left|\vec{\boldsymbol{v}} - \vec{\boldsymbol{W}}\right|\left[\frac{\vec{\boldsymbol{\omega}} \times \left(\vec{v} - \vec{W}\right)}{\omega}\right] + m\vec{\boldsymbol{g}} \tag{2}$$

where m is the mass of the projectile, $\mathbf{r}$ is the position of the projectile in Cartesian coordinates relative to the origin, $\mathbf{v}$ is the velocity of the projectile relative to the Cartesian coordinate system, ρ_A is the air density, A is the cross-sectional area of the projectile, C_D is the (dimensionless) drag coefficient, $\mathbf{W}$ is the velocity of the wind blowing relative to the same coordinate system, C_L is the (dimensionless) lift coefficient, $\boldsymbol{\omega}$ is the angular velocity of the projectile and $m\boldsymbol{g}$ is the gravitational force. Due to the highly dynamic nature of wind conditions in close proximity to the helicopter, the short range of HBT application, and the relatively large initial velocity of the projectiles, a simplification to linear trajectories is made for real time calculations. However, since all raw data is also recorded more rigorous analysis based on the data is also possible.

The azimuth, tilt, and range describe the location of the target relative to the applicator in a local spherical coordinate system centered at the applicator. In order to superimpose the local coordinates of the target over the geodetic coordinates of the applicator, the local spherical coordinates are converted into local Cartesian coordinates with a North-East-Down reference frame centered at the applicator using the following relationships:

$$x_{A\to T} = \rho \cos\varphi \cos\theta \tag{3}$$

$$y_{A\to T} = \rho \cos\varphi \sin\theta \tag{4}$$

$$z_{A\to T} = \rho \sin\varphi \tag{5}$$

where x, y, and z (with subscript A→T) designate the components of the vector from applicator to target in local Cartesian coordinates and ρ, θ and φ describe the vector in local spherical coordinates. The short range of an HBT application relative to the radius of the Earth allows for simplified calculations using a local flat surface projection. The final target offset coordinates are calculated from the following relationships:

$$\phi_T = \phi_A + \frac{x_{A\to T}}{R_{Earth}} \tag{6}$$

$$\lambda_T = \lambda_A + \frac{y_{A\to T}}{R_{Earth}\cos\phi_A} \tag{7}$$

$$h_T = h_A + z_{A\to T} \tag{8}$$

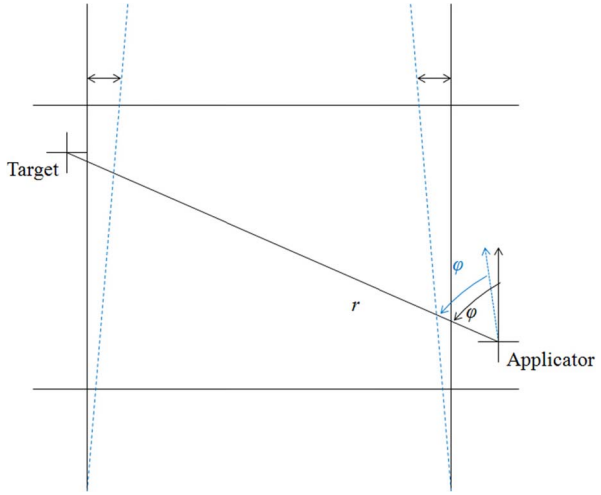

Fig. 3. Errors due to assumptions of flat surface projection (black arrows) include discrepancies of the azimuth and longitude that are dependent on the latitude. Blue dashed lines represent the actual "lines" of constant longitude that converge as latitude increases.

where ϕ, λ and h are geodetic coordinates (with subscripts T for target or A for applicator) and R_{Earth} is the radius of the Earth [16].

The flat surface approximations result in latitude-dependent errors in the estimated values of the azimuth to and longitude of the target (Fig. 3). Using the prefix "Δ" to designate the error in a parameter, errors in the target geodetic coordinates can be estimated from basic uncertainty analysis assuming that errors in each measurement are random and independent:

$$\Delta\phi_T \approx \sqrt{(\Delta\phi_A)^2 + (\xi_\phi(\phi_A))^2} \tag{9}$$

$$\Delta\lambda_T \approx \sqrt{(\Delta\lambda_A)^2 + \left(\xi_\lambda(\phi_A)\right)^2} \tag{10}$$

$$\Delta h_T = \sqrt{(\Delta h_A)^2 + (\Delta\rho\cos\varphi)^2 + (\rho\sin\varphi\,\Delta\varphi)^2} \tag{11}$$

where $\xi(\phi_A)$ is the error due to the flat surface approximation as a function of the applicator's latitude. Due to the short range of the HBT application relative to the radius of the Earth, $\xi(\phi_A)$ is relatively small compared to the horizontal and vertical errors in the GPS receiver. For example, at the approximate latitude of 20.8°, where these tests were conducted, with a range of 30 m and azimuth at 45°, the value of $\xi(\phi_A)$ is less than 10^{-6}° based on comparison with the more rigorous Vincenty formulae using the WGS-84 model, equivalent to about 0.1 m [17].

2) Microcontroller: Machine code was generated using the Arduino IDE (Arduino, Torino, Italy), and programmed onto the microcontrollers (ATMEGA328P-MUR) using software (Atmel Studio 6.1) and programming hardware (AVRISP-mkII) from the manufacturer (Atmel). During normal operation, the microcontroller polls all of the sensors for new data each cycle of the program. Any new data is sent to a paired Google Nexus 7 tablet (Asus Computer International, Fremont, CA) over Bluetooth. Each set of data is preceded by a code uniquely identifying the type of data being sent (i.e. orientation, tilt, altitude, projectile discharge, or acquisition of new target) so that the Android Bluetooth Service can parse the incoming data and update the user interface appropriately.

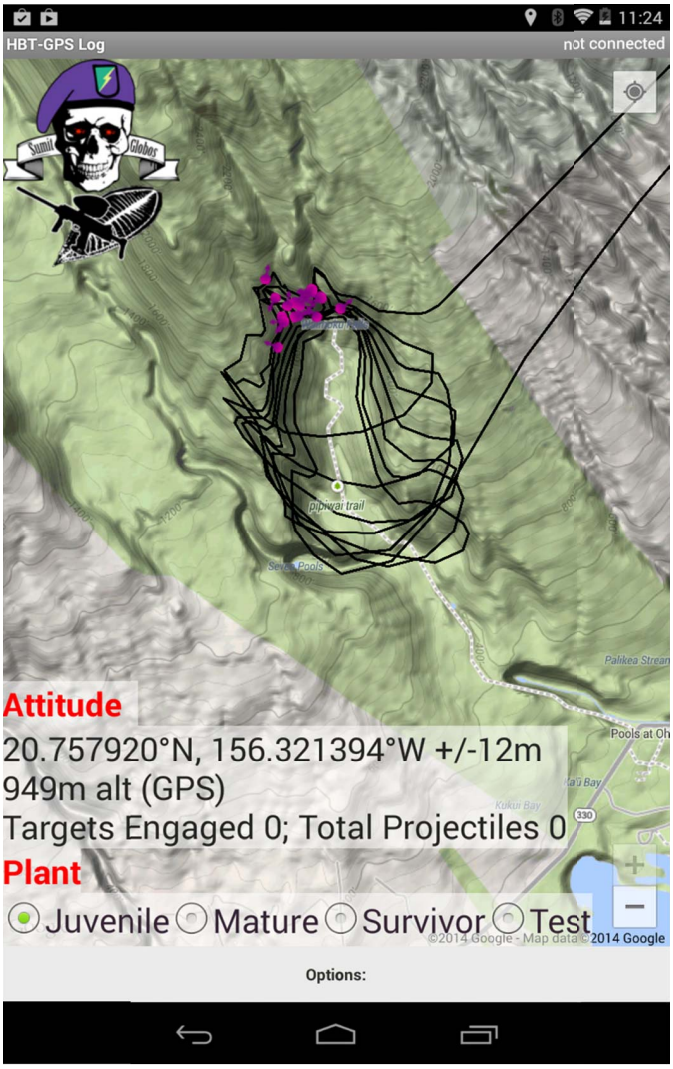

Fig. 4. User interface showing flight path and trajectories of projectiles for a single HBT operation (note that the HBT-LS is not connected so that marker orientation is not displayed, and target and projectile counts are reset to zero). Options available through the options button include connecting or disconnecting to logger over Bluetooth, starting or ending a record of data, e-mailing or displaying recorded data on the map, and launching other activities such as system calibration.

In addition, each batch of data is followed by a custom check code to validate correct transmission of data. Any data that does not contain a valid code and a correct check code is discarded by the Android device without further action. Because data is continuously streamed to the Android device and only the most recent data is recorded to associate with periodic trigger pulls and trackpoints, no attempt to recover incomplete data strings is made.

3) User Interface: An Android device is used to record data, allow the user to send commands (i.e. for calibration) to the microcontroller, and to display device data in real time both textually and on a map (Fig. 4). The custom Android application was developed using the Eclipse IDE to record GPS coordinates, parse incoming Bluetooth data transmitted from the custom hardware, record all data to a comma-delimited file, and update the user interface (with textual and map information) in real-time. An options menu on the main activity interface allows the user to connect

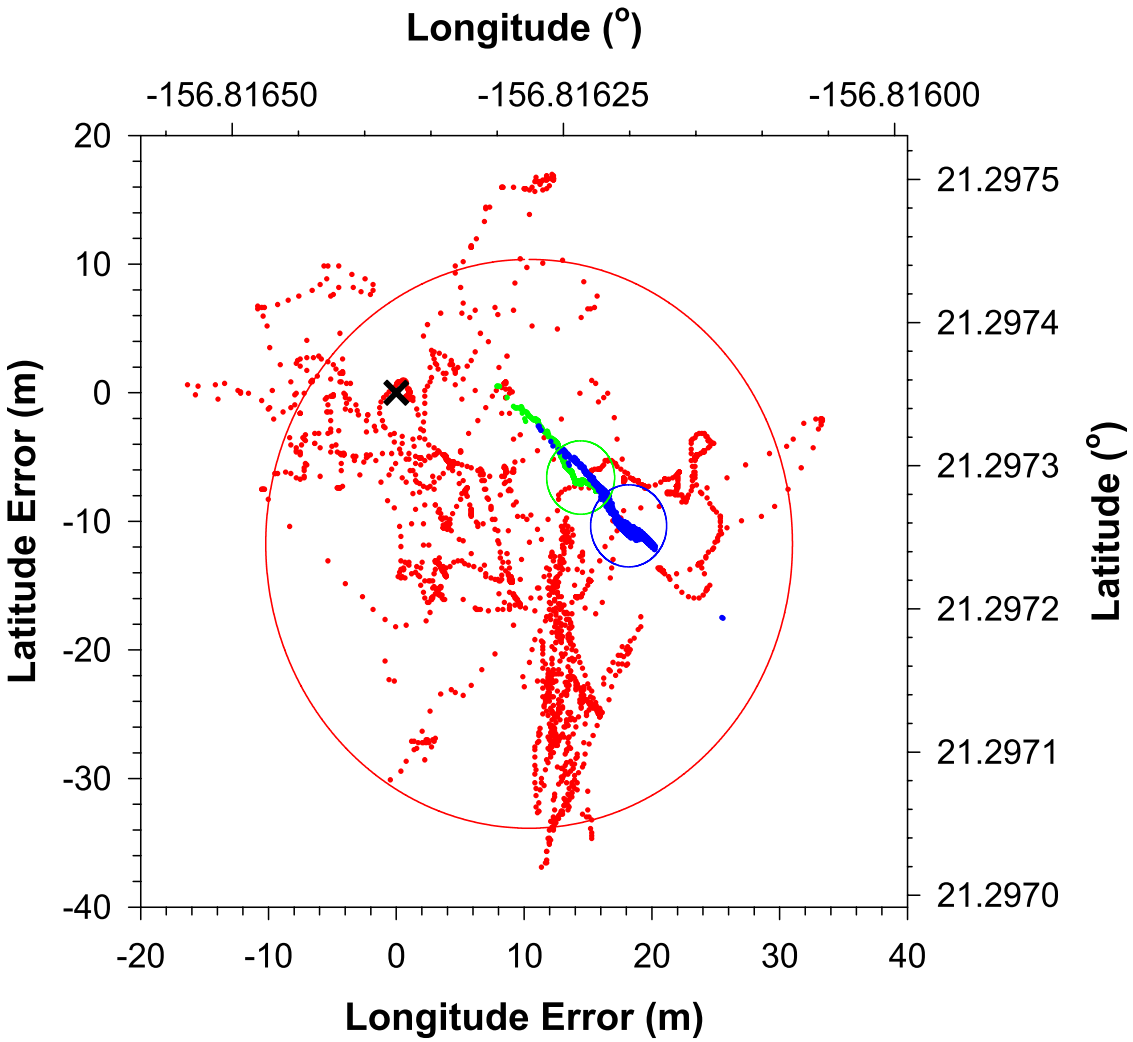

Fig. 5. Predicted locations and associated CMAS for Foretrex 401 (red), Google Nexus 7 (green) and HBT-LS (blue). Reference antenna location is marked with a black X at the origin.

wirelessly to different custom hardware, start and end data logging, display recorded data on the map, or launch other activities such as the calibration options described previously.

IV. Static Accuracy and Precision of HBT-LS

According to the National Standard for Spatial Data Accuracy (NSSDA), the accuracy of a GPS receiver is determined by root mean square error (RMSE), which is the square root of the average of the sum of the squared differences between the coordinate values from a GPS receiver relative to another more accurate source of the same position used as a reference position [18], [19].

Precision of a GPS receiver in the horizontal x and y directions (aligning respectively with lines of constant longitude and latitude), is described by the circular map accuracy standard (CMAS), which is based on the US National Map Accuracy Standards specifying that "no more than 10% of the points in the dataset will exceed a given error" [20]. Therefore, the CMAS is defined as the magnitude of the radius of the smallest circle containing 90% of the recorded positions.

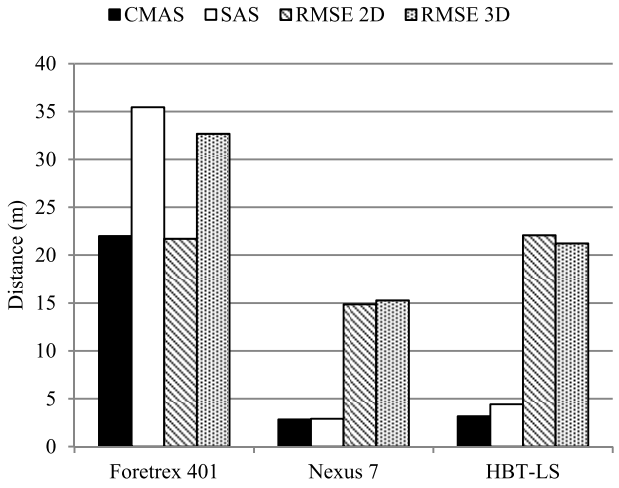

Fig. 6. Accuracy and precision statistics for Foretrex 401, Google Nexus 7 and HBT-LS.

Assuming normally distributed errors in the horizontal coordinates CMAS can be described mathematically as

$$CMAS = 2.1460\sigma_c \tag{12}$$

TABLE I
HERBICIDE DOSES (GRAMS OF ACID EQUIVALENT TARGET^{-1}) DERIVED FROM HBT-LS COMPARED TO COMPOSITE AVERAGES

Date	03/27	04/22	04/23	04/24	05/08	05/09	05/20
Targets[a]	142	97	49	40	2	13	37
Mean[b]	3.39	4.04	7.21	9.60	14.46	11.40	5.92
±SD[c]	2.40	2.80	6.26	7.34	4.37	1.39	3.58
Avg_{comp}[d]	3.68	3.95	6.86	8.84	17.55	12.27	7.02
Δ(%)[e]	8.0	2.4	5.0	8.2	19.3	7.4	16.9

[a] Number of targets treated during operation
[b] Mean herbicide dose derived from HBT-LS assignment to individual projectiles
[c] Standard deviation of herbicide dose derived from HBT-LS
[d] Average composite derived from the total number of pods consumed (~160 projectiles each) divided the total number of targets treated in each operation
[e] Percent difference between mean herbicide use determined based on HBT-LS usage statistics and average composite

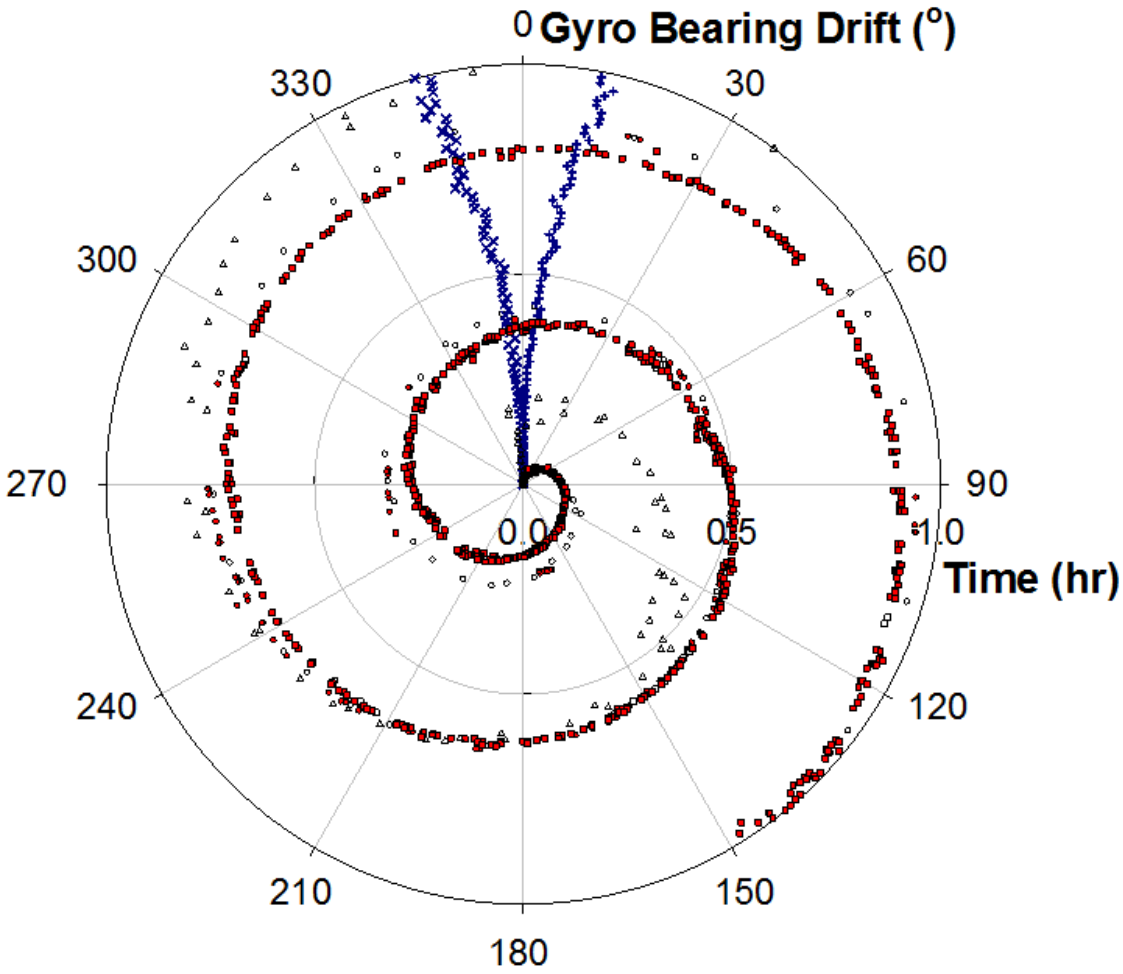

Fig. 7. Deviation in gyroscope bearing with respect to compass bearings (in degrees) over time, for stationary logger unit with sensor z axis (×) or y axis (+) aligned with vertical/gravitational force, or recorded under dynamic conditions over the course of three separate airborne operations (circles, squares, and triangles). Symbols without fill are trackpoint data during aerial operations, and red filled symbols are associated with projectile discharges. To remove clutter data was decimated leaving only every 10th data point.

where the circular standard error σ_c can be approximated by

$$\sigma_c \sim \frac{1}{2}\left(\sigma_x + \sigma_y\right) \tag{13}$$

where σ_x and σ_y are the standard deviations in horizontal position corresponding to errors in latitude and longitude, respectively, assuming that the larger of two is less than 5x the magnitude of the other [21].

Precision of a GPS receiver in three dimensions, including the z (vertical) direction, is given by the Spherical Accuracy Standard (SAS), which is defined as the magnitude of the radius of the smallest sphere containing 90% of the recorded positions. This value can be estimated as

$$SAS = 2.5\sigma_s \tag{14}$$

where σ_s is the spherical standard error approximated by

$$\sigma_s \sim \frac{1}{3}\left(\sigma_x+\sigma_y+\sigma_z\right) \quad (15)$$

where σ_z is the standard deviation in altitude, assuming that the smallest of the three component standard deviations is not less than 0.35x the magnitude of the largest [21].

On July 20, 2014, calibrations were performed with the HBT-LS and other consumer-grade GPS receivers against a GPS reference station (Trimble NetRS: 21° 17′ 50.46″ N, 157° 48′ 58.95″ W, 81.378m above sea level) located in Honolulu, HI. The consumer-grade GPS units calibrated in this study included a Google Nexus 7 tablet independent of the HBT-LS and the Foretrex 401 handheld (Garmin Olathe, KS). These GPS units were placed at the base of the reference station antenna on the roof and their positions recorded every 5 seconds for 3 hours. With the sensor board mounted to the marker, the HBT-LS was mounted in an articulated vise (PanaVise 350, Reno, NV) at a horizontal distance of approximately 18 meters from and aligned azimuth to target the reference position with azimuth 290°. In this attitude data was recorded by the HBT-LS every 5 seconds for 3 hours. Accuracy for all test receivers was determined by RMSE relative to the known reference position, while precision was determined by radial magnitudes for CMAS and SAS as described above. The reference position was estimated from HBT-LS data using the known distance to target to completely define the vector from marker to the reference.

V. Dynamic Accuracy and Precision in Operations

Aerial surveillance operations were conducted in 2014 targeting *Miconia calvescens* and *Psidium cattleianum* weed populations on Maui with the HBT-LS integrated to the electro-pneumatic marker. Operations were conducted using a Hughes 500D helicopter with the applicator positioned on the port side behind the pilot as described by Leary et al. [10]. In these operations, the HBT-LS recorded all projectiles discharged with timestamp and target assignment along with all other calibrated sensor information. Operational data were evaluated to determine the distribution of projectile trajectories with respect to the nose of the aircraft and the horizontal plane.

For a data subset (n = 362) an additional HBT-LS was positioned at the nose for calculation of the angle between the applicator and aircraft azimuths and bearing for comparison with the horizontal target window (i.e., 270° to 330°) corresponding to the shared view of the pilot and applicator. Tilt values were compared to the vertical target window (i.e., 0° to −50°). Altitude above ground level (Alt_{agl}) was estimated as the difference between the elevation inferred from the barometric pressure readings and the raster pixel value of the digital elevation model (DEM; 10m resolution) corresponding to the recorded point location.

Herbicide dose accuracy was measured as the percent difference between mean target dose rate recorded by HBT-LS (average number of projectiles used to treat each unique target ID) and composite averages in each operation estimated by dividing the total number of pods (projectile containers) consumed (∼160 projectiles per pod) by the total number of targets treated in an operation, with rounding errors expected [9].

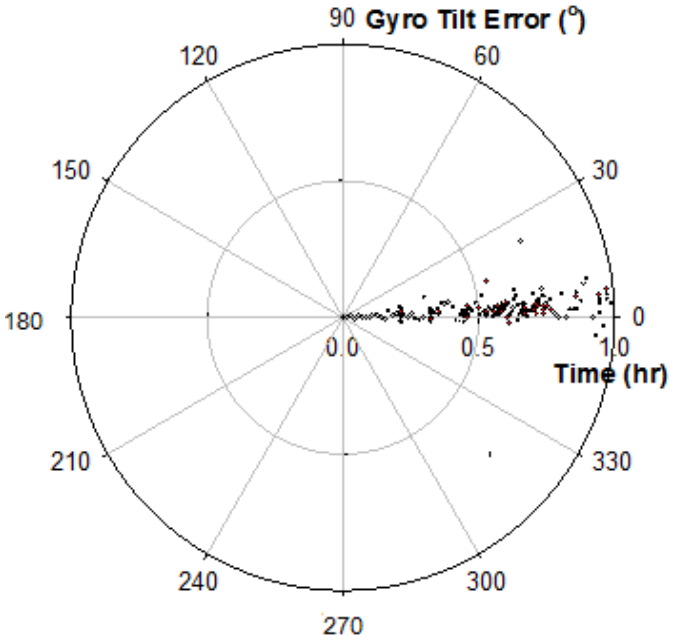

Fig. 8. Deviation in tilt estimate from gyro with respect to tilt estimate from compass, for data in a single aerial operation. Red filled symbols are data associated with a projectile discharge, and unfilled symbols are from trackpoint data. Data are decimated to show only every 10th data point to remove clutter.

VI. Results

A. Accuracy and Precision of Target Coordinates

Both HBT-LS and tablet exhibited static circular and spherical precisions about seven times smaller than the corresponding values recorded for the handheld GPS unit (Fig. 5). Accuracy (RMSE) of the tablet was also superior to the other GPS unit in 2D and 3D, while the HBT-LS was superior to the handheld GPS in 3D accuracy (Fig. 6). Moreover, it is worth noting how the BCM4751 receivers of the HBT-LS and tablet were coinciding with much more stable plots of the coordinates in the short three hour period compared to the widely dispersed random appearance of the handheld GPS (see Fig. 6). The HBT-LS points are shifted further from the reference point, which is likely due to compounding errors exhibited by the tilt and azimuth sensors used for determining the target location and approximations made in installation and offset calculation.

B. Operational Validation

The HBT-LS successfully acquired data from seven independent operations in 2014 for a total of 11,132 projectiles assigned to 400 targets. Android tablets never became disconnected, textual data displayed on the app was constantly refreshed during operations, and the system was never observed to miss a trigger pull during operation, suggesting that the data communication was robust. By assigning target IDs to each projectile with the HBT-LS, we were able to qualitatively identify the target dose outliers (i.e., a large target

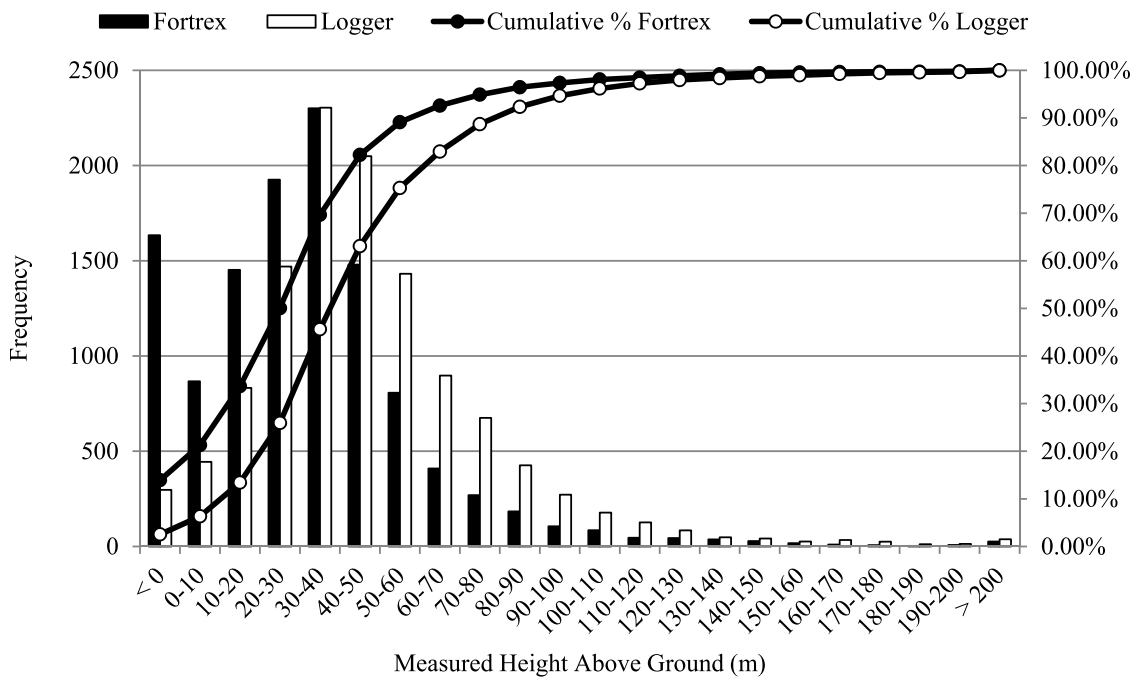

Fig. 9. Altitude above ground at the point of application estimated from elevation measurements from the HBT-LS (n = 11, 724) and Foretrex 401 (n = 11, 745) with ground level inferred from a 10-m digital elevation model at the recorded location.

treated with large projectile quantity) and also calculate mean values with standard deviations for each operation (Table I). In total, the HBT-LS mean (± standard deviation) calculations were within 11% of the composite estimated values. Anecdotally, herbicide dose corresponds to weed target size, so that HBT application data can be useful for assessing population age and phenology across the geographical range of operations. The standard deviations observed in this data set were rather large relative to the mean, suggesting diverse target populations. The capability of generating standard deviations will enhance interpretations with measures of uniformity and for segregating target outliers based on size class.

Efforts to determine the accuracy of the azimuth offset relative to the target window deduced from the track vector bearing were prone to large errors, particularly when the aircraft was in a stationary hover and pivoting on its axis (data not shown) such that the track direction did not coincide with the aircraft orientation. Despite a large interquartile range, the most frequent azimuth offset estimated for applicator relative to aircraft nose under these conditions was 311°. Vertical tilt estimates, on the other hand, were independent of aircraft bearing and so had a much tighter interquartile range of −20° to −41°. The more limited azimuth data subset relative to aircraft orientation recorded simultaneously by a separate logger in the cockpit displayed an interquartile range from 292° to 335°, contained within the perceived target window.

The average time on target (time interval between the first and last projectile discharged) was 12.3 ± 9.8 s.

To determine the stability of the gyroscope readings of azimuth and tilt (relative to those from the digital compass readings) were recorded both under static and dynamic conditions, and plotted against time (Figs. 7 and 8 respectively). Stationary data indicated that gyroscope readings have small axis-dependent biases in rotational velocity, which does not completely explain the relatively large systematic drift observed during aerial operations. Furthermore, the systematic drift experienced during aerial operations is not explained by random integration errors in the digital motion processor on the MPU-6050. This suggests that vibration or other motion artifacts might superimpose significant biases onto the rotational velocity measurements around the vertical axis, for example by inducing sympathetic vibrations in the gyroscope oscillators at odd harmonics. The deviation in tilt is not subject to this systematic drift, as the digital motion processor in the gyroscope chip corrects for drift in the tilt measurements based on acceleration (gravity) measurements in the different axes. No systematic drift was observed in stationary measurements of the digital compass. In addition, compass bearing to targets in operational data corresponded closely to expectations in that application is primarily against weed targets populating cliffsides, so that trajectories were more or less perpendicular to contours of terrain maps in the direction of increasing elevation. These data suggest that the aircraft did not significantly distort or shield local geomagnetic fields, and that at least in the areas of our operations there are little if any local distortions in the field.

The $\mathrm{Alt_{agl}}$ values (applicator elevation estimated from barometric pressure relative to ground surface elevation estimated for the corresponding GPS position on 10m digital elevation model) estimated from operational data recorded from the HBT-LS and consumer-grade GPS, were highly variable and included some negative values (Fig. 9). It should also be noted that some dramatic weather changes occurred during several of the operations which likely confounded many of the altimeter

estimates based on the calibrated barometric pressure at the start of operations and correspondingly contributed to errors in Alt_{agl}.

VII. Conclusion

The HBT-LS provided satisfactory accuracy and precision relative to consumer-grade handheld GPS units currently in use, enhanced data acquisition with new spatial and quantifiable attributes, while maintaining a low profile relative to the marker. Testing in an operational setting showed that results are consistent with anecdotal observation and expectations. Improvements in altimeter recordings may be necessary for better determination of offset locations to targets. Implementation of laser rangefinders to determine the range to the plant target and altitude will further improve the utility of the logger and enable direct estimation of target location without requiring knowledge of elevation and reference to digital elevation maps. Use of a single chip 9 axis sensor and additional sensor fusion between the accelerometer, gyroscope and magnetic compass for improved bearing determination should also be implemented. While this system was developed for use with the HBT platform, alternative applications include the use of marking agents to track the positions of plants and animals, including invasive species or livestock, surveying difficult to reach terrain, and spatial analysis of video and still imagery recorded by UAVs.

Acknowledgment

The authors would like to thank Dr. J. Foster and the Pacific GPS Facility for allowing use of their GPS reference station for accuracy and precision experiment.

References

[1] G. W. Cox, *Alien Species in North America and Hawaii*, 1st ed. Washington, DC, USA: Island Press, 1999.

[2] L. Loope and F. Kraus, "Preventing establishment and spread of invasive species: Current status and needs," in *Conservation of Hawaiian Forest Birds: Implications for Island Birds*, New Haven, CT, USA: Yale Univ. Press, 2009.

[3] L. Loope, F. Starr, and K. Starr, "Protecting endangered plant species from displacement by invasive plants on Maui, Hawaii," *Weed Technol.*, vol. 18, pp. 1472–1474, Dec. 2004.

[4] H. A. Mooney and J. A. Drake, "Ecology of biological invasions of North America and Hawaii," in *Ecological Studies: Analysis and Synthesis*. Berlin, Germany: Springer-Verlag, 1986.

[5] C. P. Stone and J. M. Scott, *Hawaii's Terrestrial Ecosystems: Preservation and Management*, 1st ed. Honolulu, HI, USA: Univ. Hawaii Press, 1985.

[6] C. P. Stone, C. W. Smith, and J. T. Tunison, *Alien Plant Invasions in Native Ecosystems of Hawaii: Management and Research*. Honolulu, HI, USA: Univ. Hawaii Press, 1992.

[7] D. B. Lindenmayer, C. R. Margules, and D. B. Botkin, "Indicators of biodiversity for ecologically sustainable forest management," *Conserv. Biol.*, vol. 14, no. 4, pp. 941–950, 2000.

[8] C. Kueffer and L. Loope, "Prevention, early detection and containment of invasive, nonnative plants in the Hawaiian Islands: Current efforts and needs," Dept. Botany, Univ. Hawaii at Manoa, Honolulu, HI, USA, Tech. Rep. 166, Aug. 2009.

[9] J. J. K. Leary, J. Gooding, J. Chapman, A. Radford, B. Mahnken, and L. J. Cox, "Calibration of an herbicide ballistic technology (HBT) helicopter platform targeting *Miconia calvescens* in Hawaii," *Invasive Plant Sci. Manage.*, vol. 6, no. 2, pp. 292–303, Jan. 2013.

[10] J. J. K. Leary *et al.*, "Reducing nascent miconia *(Miconia calvescens)* patches with an accelerated intervention strategy utilizing herbicide ballistic technology," *Invasive Plant Sci. Manage.*, vol. 7, no. 1, pp. 164–175, Jan. 2014.

[11] J. S. Jang and D. Liccardo, "Automation of small UAVs using a low cost MEMS sensor and embedded computing platform," in *Proc. IEEE/AIAA 25th Digital Avionics Syst. Conf.*, Oct. 2006, pp. 1–9.

[12] M. Steen, P. M. Schachtebeck, M. Kujawska, and P. Hecker, "Analysis and evaluation of MEMS INS/GNSS hybridization for commercial aircraft and business jets," in *Proc. IEEE/ION Position Location Navigat. Symp. (PLANS)*, May 2010, pp. 1264–1270.

[13] J. Kolecki and P. Kuras, "Low cost attitude and heading sensors in terrestrial photogrammetry—Calibration and testing," *Archiwum Fotogrametrii, Kartografii Teledetekcji*, vol. 22, pp. 249–260, 2011.

[14] G. Troni and L. L. Whitcomb, "Preliminary experimental evaluation of in-situ calibration methods for MEMS-based attitude sensors and Doppler sonars in underwater vehicle navigation," in *Proc. IEEE/OES Auto. Underwater Veh. (AUV)*, Sep. 2012, pp. 1–8.

[15] G. Robinson and I. Robinson, "The motion of an arbitrarily rotating spherical projectile and its application to ball games," *Phys. Scripta*, vol. 88, no. 1, p. 018101, Jul. 2013.

[16] B. L. Decker, "World Geodetic System 1984," Defense Mapping Agency Aerospace Center, St. Louis, Mo, USA, Accession No. ADA167570, Apr. 1986.

[17] T. Vincenty, "Direct and inverse solutions of geodesics on the ellipsoid with application of nested equations," *Surv. Rev.*, vol. 23, no. 176, pp. 88–93, 1975.

[18] Federal Geographic Data Committee, "National standard for spatial data accuracy (NSSDA)," Federal Geographic Data Committee, Washington, DC, USA, Tech. Rep. FGDC-STD-007.3-1998, 1998.

[19] *Information Technology—Spatial Data Transfer Standard*, ANSI-NCITS Standard 320:1998, Jun. 1998.

[20] *United States National Map Accuracy Standards*, U.S. Bureau Budget, Washington, DC, USA, 1947.

[21] C. R. Greenwalt and M. E. Shultz, *Principles of Error Theory and Cartographic Applications*. St. Louis, MO, USA: Aeronautical Chart and Information Center, 1965.

Roberto Rodriguez, III (M'14) received the B.S. degree in biological engineering from the University of Hawaii at Manoa, Honolulu, HI, USA, where he is currently pursuing the M.S. degree in biological engineering.

He has been a Research Assistant with the Department of Molecular Biosciences and Biological Engineering, University of Hawaii at Manoa, since 2013, and a member of the American Society of Agricultural and Biological Engineers since 2014. His current research interests include the use of remote sensing for environmental and medical applications.

Daniel M. Jenkins received the B.S. and M.Eng. degrees in agricultural and biological engineering from Cornell University, Ithaca, NY, USA, in 1995 and 1996, respectively, and the Ph.D. degree in biological and agricultural engineering from the University of California at Davis, Davis, CA, USA, in 2001.

He has been a faculty member with the Department of Molecular Biosciences and Bioengineering, University of Hawaii at Manoa, Honolulu, HI, USA, since 2002, a member of the American Society of Agricultural and Biological Engineers since 1998, and a member of the American Chemical Society since 2005. His primary interest is in molecular and other sensor systems for agricultural and environmental applications.

James J. K. Leary received the B.S. degree in horticulture with a minor in chemistry from Michigan State University, East Lansing, MI, USA, in 1996, and the M.S. degree in horticulture and the Ph.D. degree in molecular biosciences and biological engineering with a specialization in weed science and molecular ecology from the University of Hawaii at Manoa, Honolulu, HI, USA, in 1999 and 2006, respectively.

He has served as a faculty member with the Department of Natural Resources and Environmental Management, University of Hawaii at Manoa, since 2009, where he ranked as an Assistant Specialist with a research and extension split appointment. His interests are applied research in invasive plant species management.

Reducing Nascent Miconia (*Miconia calvescens*) Patches with an Accelerated Intervention Strategy Utilizing Herbicide Ballistic Technology

James Leary, Brooke V. Mahnken, Linda J. Cox, Adam Radford, John Yanagida, Teya Penniman, David C. Duffy, and Jeremy Gooding*

The miconia (*Miconia calvescens*) invasion of the East Maui Watershed (EMW) started from a single introduction over 40 yr ago, establishing a nascent patch network spread across 20,000 ha. In 2012, an accelerated intervention strategy was implemented utilizing the Herbicide Ballistic Technology (HBT) platform in a Hughes 500D helicopter to reduce target densities of seven nascent patches in the EMW. In a 14-mo period, a total of 48 interventions eliminated 4,029 miconia targets, with an estimated 33% increase in operations and 168% increase in recorded targets relative to the adjusted means from 2005 to 2011 data (prior to HBT adoption). This sequence of interventions covered a total net area of 1,138 ha, creating a field mosaic of overlapping search coverage (saturation) for each patch (four to eight interventions per patch). Target density reduction for each patch fit exponential decay functions ($R^2 > 0.88$, $P < 0.05$), with a majority of the target interventions spatially assigned to the highest saturation fields. The progressive decay in target density led to concomitant reductions in search efficiency (min ha^{-1}) and herbicide use rate (grams ae ha^{-1}) in subsequent interventions. Mean detection efficacy (± SE) between overlapping interventions ($n = 41$) was 0.62 ± 0.03, matching closely with the probability of detection for a random search operation and verifying imperfect (albeit precise) detection. The HBT platform increases the value of aerial surveillance operations with 98% efficacy in target elimination. Applying coverage saturation with an accelerated intervention schedule to known patch locations is an adaptive process for compensating imperfect detection and building intelligence with spatial and temporal relevance to the next operation.

Nomenclature: Miconia, *Miconia calvescens* DC.

Key words: Adaptive management, aerial surveillance, GIS, nascent patch network, random search operation, mortality factor.

An exotic plant invasion is a phenomenon carried out by species with the capability to occupy niches already inhabited by other indigenous or endemic plant communities (Richardson et al. 2000). This invasion phenomenon is also a main driver in habitat fragmentation, leading to modification of an ecosystem's structure and function (Gilbert and Levine 2013). The resultant loss of endemic biological diversity is particularly detrimental for isolated island ecosystems that exhibit high endemism (Denslow 2003; Mack et al. 2000; Reaser et al. 2007).

A commitment to weed species eradication starts with an effective containment strategy targeting the nascent patch network that is expanding the invasion front (Cousens and Mortimer 1995; Moody and Mack 1988; Rejmánek and Pitcairn 2002). Reconnaissance and surveillance are fundamental activities for nascent weed detection and spatial delimitation (Baxter and Possingham 2011; Cacho et al. 2007; Hester et al. 2010; Lawes and McAllister 2006; Panetta and Lawes 2005; Rew et al. 2006; Taylor and Hastings 2004). Reconnaissance tends to be a more cursory

DOI: 10.1614/IPSM-D-13-00059.1

* First, third, and fifth authors: Assistant Specialist, Specialist and Professor Department of Natural Resources and Environmental Management, University of Hawaii at Manoa, Honolulu, HI 96822; second, fourth, and sixth authors: GIS Specialist, Operations Manager and ManagerMaui Invasive Species Committee, University of Hawaii at Manoa, Honolulu, HI 96822; seventh author: Director Pacific Cooperative Studies Unit, University of Hawaii at Manoa, Honolulu, HI 96822; eighth author, Liaison Pacific Islands Exotic Plant Management Team, National Park Service Biological Resource Management Division. Current address of first author: Maui Agricultural Research Center, P.O. Box 269, Kula, HI 96790. Corresponding author's E-mail: leary@hawaii.edu

Management Implications

The herbicide ballistic technology (HBT) platform is a herbicide delivery system registered as a 24(c) Special Local Need for use in Hawaii to treat nascent satellite miconia patches in remote natural areas that require helicopter operations. We define an intervention as a weed management operation with the combined actions of target detection immediately followed by effective elimination. In 14 mo, a total of 48 interventions were conducted for seven nascent patches, (1) eliminating 4,029 miconia targets and (2) encompassing a total net area of 1,138 ha, while (3) administering $< 1\%$ of the maximum allowable herbicide use rate. Target density reduction for the patch network was $> 86\%$, fitting an exponential decay function. This resulted in a threefold improvement in search efficiency (min ha^{-1}) and a 10-fold reduction in herbicide use rate (g ae ha^{-1}). Expansion of the total net area corresponded to improvements in search efficiency; less time was needed to saturate known target locations with reduced densities. These interventions are described as random search operations with imperfect detection. Efficacy of an HBT application to miconia can be confirmed in less than 1 mo, allowing for the acceleration of intervention schedules that can compensate for imperfect detection by saturating coverage with compounding sequential interventions. The goals of this accelerated intervention strategy are to rapidly reduce nascent patch populations to manageable or undetectable levels and build spatially and temporally explicit intelligence, where expected projections are accurate with observed values.

process of searching for new target locations, whereas surveillance is distinguished by a more intensive process of building explicit intelligence on known target locations with repeated visits (Anonymous 2007). In the early stages of strategy development, reconnaissance may be a necessary trade-off to actual treatment activities when a lack of intelligence compromises a sound priority decision process (Baxter and Possingham 2011). Otherwise, surveillance is a more common practice of gathering intelligence, usually as an ad hoc activity complementary to active management and relegated to within the immediate vicinity of the management area (Cacho et al. 2007; Fox et al. 2009). Detection of invasive plant species residing in their natural settings is an imperfect process (Moore et al. 2011; Regan et al. 2011). Good intelligence, regardless of the survey design, should account for imperfect detectability as an adaptive process for optimizing future operations (Moore et al. 2011; Regan et al. 2011; Thompson 2002).

Cacho et al. (2007) coined the term ''mortality factor'' to describe management of individual weed targets, accounting for both detection and effective treatment as complementary actions necessary to achieving target elimination. With an effective treatment technique, detection then becomes the determinant outcome of an operation (Leary et al. 2013; Lodge et al. 2006). Koopman (1946) introduced the mathematical framework for estimating the probability of detection (P_d) in a random search operation that would be expected within a terrestrial environment (Cooper et al. 2003). Search impediments (i.e., topography, weather, surrounding vegetation) imposing even slight randomness in coverage (c), have been shown to fit the exponential detection function (Equation 1) as a conservative estimate of an imperfect search effort (Cacho et al 2007; Frost 1999):

$$p_d = 1 - e^{-c} \quad [1]$$

Herbicide Ballistic Technology (HBT) is a weed target intervention platform that was developed in Hawaii to enhance helicopter surveillance operations with the capability to dispatch satellite weed targets upon detection (Leary et al. 2013). The HBT platform discretely administers small-aliquot herbicide projectiles through a pneumatic application device to treat individual weed targets with long-range accuracy (i.e., 30 m [98 ft] effective range) from horizontal or vertical trajectories. It expands the capability to treat all detectable targets that might otherwise be untreatable with other conventional application methods. An effective HBT treatment application enhances surveillance operations with the full complement of a mortality factor (Leary et al. 2013).

The term ''intervention'' is used here to distinguish from other surveillance operations with the inclusion of a mortality factor accommodated by the integration of an HBT platform. This study expands on platform calibrations described by Leary et al. (2013) with the accelerated deployment of an adaptive intervention strategy targeting the primary nascent patch network of the miconia (*Miconia calvescens* DC.) invasion in the East Maui Watershed (EMW; Hawaii). We report on spatial and temporal parameters of performance measures associated with patch target density reductions incurred by these intervention sequences.

Materials and Methods

Target Species: *Miconia calvescens*. Miconia is a midstory tree, 12 to 15 m tall, native to Central and South America. It was introduced to the Hawaiian Islands in 1961 and was presumably introduced to the island of Maui by 1970, where the first management program in the state was initiated 20 yr later (Chimera et al. 2000; Medeiros et al. 1997). Miconia is an autogamous species that reaches maturity in 4 to 5 yr. A single plant has immense fecundity, producing millions of propagules in a single reproductive cycle (Meyer 1998). Its fruit are small and edible, lending itself to frugivorous dispersal by a diverse avian community (Chimera et al. 2000; Spotswood et al. 2013). In Australia, the dispersal range of a nascent patch had been estimated to exceed 2,000 m, but with 95% of the recruitment contained within 500 m of the maternal source (Hardesty et al. 2011; Murphy et al. 2008). Viable seed persistence has been measured beyond 16 yr (Meyer et al. 2011), contributing to the long-term recruitment potential of a latent seed bank.

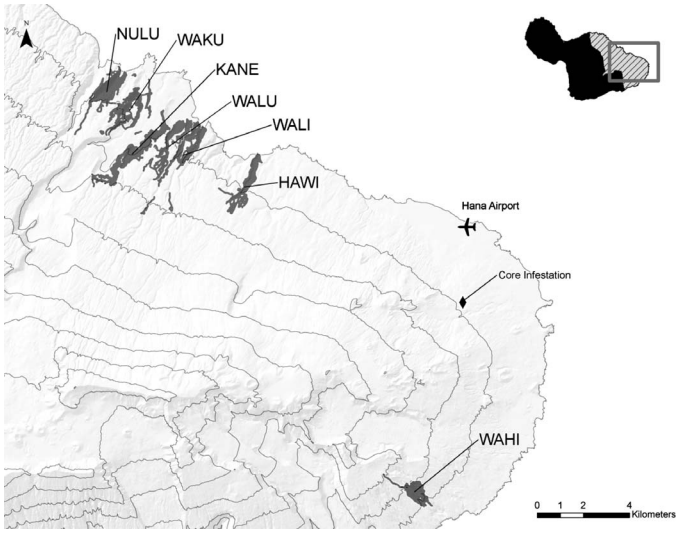

Figure 1. Map of East Maui Watershed with mean center of the miconia core infestation (CORE; black diamond) and the final net areas of the patch units (shaded buffers with corresponding four-letter acronyms; black). See Experimental Units in the Materials and Methods section. 300-m contours displayed on the base map.

Suitable Habitat: The EMW. The EMW encompasses over 55,000 ha (136,000 ac) on the windward slope of Haleakala Crater on Maui. The core miconia infestation occupies < 1,000 ha on the easternmost portion of EMW (20°47′44″N, 156°00′52″W), while the spatial distribution of the nascent patch network is spread across an estimated 20,000 ha (Figure 1). The invasion is below 1,000 m above sea level (m_{asl}) with invasion fronts advancing south 8 km (5 mi) and west 18 km from the core infestation (CORE), respectively. The mean annual precipitation range within this area is 3,000 to 6,000 mm (118–236 in) (Giambelluca et al. 2013). The mean annual temperature from Hana Airport (24 m_{asl}) is 23.4°C (74.1 F; 1950 to 2005; WRCC 2013) with a lapse rate of −0.64°C per 100 m elevation (Jacobson 2005). These climatic conditions are consistent with the description of a suitable habitat in French Polynesia (Pouteau et al. 2011). The dominant vegetation types include a wet coastal forest with mixed exotic canopy species (e.g., African tulip tree [*Spathodea campanulata* P. Beauv.], eucalyptus [*Eucalyptus robusta* Sm.], guava [*Psidium* spp.]) that transitions to a wet montane forest at higher elevations, represented by endemic assemblages (e.g. ohi'a [*Metrosideros polymorpha* Gaudich] and koa [*Acacia koa* Gray]) (Wagner et al. 1999) that also serve as critical habitat for 59 other threatened and endangered plant species (Anonymous 2000). Miconia is capable of invading EMW critical habitat above 1,000 m_{asl} (Medeiros et al. 1997; Meyer 1996; Meyer and Florence 1996; Pouteau et al. 2011), making mitigation of its spread into these areas a strategic priority.

Over the last decade, systematic surveys of the entire watershed have identified all major nascent patch populations along with hundreds of incipient satellites. These patches are comparably smaller and phenologically distinguishable from the CORE, with plant maturity observed less frequently. They are most often identified as juvenile understory saplings (ca. < 3 m tall) that may be aggregating into monotypic midstory canopies. These patches also tend to colonize the extreme topography associated with the ravines and drainages of EMW's heterogeneous landscape (see Pouteau et al. 2011 for similar topographic features).

Experimental Units: The Miconia Patch Network. Seven of the most prominent patches within the network were selected to test an accelerated intervention schedule (see below): Nuuailua (NULU), Waiakuna Pond (WAKU), Keanae Wall (KANE), Wailua nui (WALU), Wailua iki (WALI), Hanawi (HAWI), and Waihiumalu (WAHI) (Figure 1). Five of the patches (NULU, WAKU, KANE, WALU, and WALI) were located along the western front of the invasion, 12 to 18 km from the CORE. Each of the western-front patches was within a 1,000-m radius of the next adjacent patch, creating a viable interpatch network for frugivorous dispersal (Hardesty et al. 2011; Murphy et al. 2008). The HAWI patch was approximately 3,000 m from the nearest patch (WALI). However, several targets interspersed between these patches had been dispatched in separate operations that were not a part of this study. The WAHI patch was located on the southern front of the invasion and was closest to the CORE (ca. 8 km from centers). One other known patch was just south of WAHI, and was also being managed independently of this study.

The Accelerated Intervention Schedule. The strategy implemented for this study consisted of an accelerated deployment schedule of sequential interventions. A total of 48 interventions were conducted on eight separate dates over a 14-mo period, with all patches receiving at least four interventions and three of the seven receiving eight interventions (Table 1). The time intervals between interventions ranged from 18 to 182 d with the median/mode interval at 32 d. Based on previous recorded operations conducted in these patch areas (2005 to 2011), the intervention schedules for this study were accelerated by 33% (Supplemental Table 1, http://dx.doi.org/10.1614/IPSM-D-13-00059.TS1). All helicopter operations were conducted with a full fuel load, providing 70 to 100 min of operation flight time. Starting locations were typically at the lowest elevation point for each patch, proceeding with an adaptive process of deliberating search efforts to known target locations based on intelligence derived from previous interventions (Fox et al. 2009; Thompson 2002). Any remaining flight time would accommodate expansion of search coverage to surrounding adjacent areas, typically into higher elevations. Flight lines were anisotropic, running

Table 1. Intervention data recorded for the seven nascent miconia patches.

Patch	Intervention[a]	Gross area[b] (ha)	Net area[c] (ha)	Targets	OFT[d] (min)	PC[e]
HAWI	4	302.0	130.8	471	574.1	14,698
WAHI	6	275.8	94.4	465	574.3	11,431
WAKU	7	329.1	194.0	412	562.8	12,167
WALI	7	478.1	175.0	401	684.9	14,127
WALU	8	412.9	154.4	676	764.7	17,174
NULU	8	586.7	174.6	508	785.8	14,294
KANE	8	688.8	214.9	1096	1169.8	31,674
NETW[f]	48	3073.4	1138.1	4029	5116.4	115,565

[a] Interventions conducted in February 2012, May 2012, June 2012, October 2012, November 2012, December 2012, February 2013, March 2013, and April 2013.

[b] Momentary gross area.

[c] Cumulative net area.

[d] Abbreviations: OFT, operation flight time; PC, projectile consumption; HAWI), Hanawi; WAHI, Waihiumalu; WAKU, Waiakuna Pond; WALI, Wailua iki; WALU, Wailua nui, NULU, Nuuailua; KANE, Keanae Wall; NETW, network.

[e] Projectile consumption estimated from the pod inventory (ca. 140 projectiles pod^{-1}).

[f] Total values for the entire patch network.

along the contours of the steep topography and with iso-altitudinal transects spaced $<$ 50 m of elevation apart for ensuring visual search overlap from valley floor to ridgeline.

Helicopter HBT Platform and Intervention Procedures. All aerial operations were conducted in a Hughes 500D helicopter by a three-person crew with a portside bias creating a 210° field of view and a detectable sight range estimated at 50 m. Operation speeds were maintained at $<$ 20 km h^{-1} while actively searching. Miconia targets were treated with 17.3-mm soft-gel projectiles encapsulating 199.4 mg ae (0.007 oz) of the active herbicide ingredient triclopyr. Applicators administered three to five projectiles to each stem axial point (e.g., larger targets with more axial points received higher doses). The applicator, seated portside behind the pilot, administered an effective herbicide dose to target within a 30-m effective range. Operation data were recorded with a Fortrex® 301 global positioning system (GPS) data logger (Garmin®; Olathe, KS) with flight lines recorded as 5-sec vertex track logs and dispatched targets recorded as waypoints, which were actually recorded from the position of the application and not the actual location of the target (i.e., within 30 m). This protocol was consistently applied to all recorded points due to flight safety considerations. Projectile consumption was determined at the end of each operation. For further details on these protocols refer to Leary et al. (2013).

Geographic Information System Data Analyses. All GPS data were projected in the NAD 1983 UTM Zone 4N coordinate system and processed in ArcMAP® 10.1 (Esri®; Redlands, CA). Tracks logs were manually spliced into operation flight segments that were $\leq$ 16 km h^{-1}. Search coverage areas were calculated from these operation flight segments using buffer tool procedures with a full 50-m radius and dissolved overlap. Operation times were calculated by tabulating the number of vertices in these same flight segments (e.g., 12 vertices min^{-1}). All buffers for each patch were superimposed with a union tool procedure creating a field mosaic of the cumulative net area. Coverage saturation levels for each field were scored by the number of overlapping buffers. As an example, an area mosaic created by eight interventions contained fields representing all levels of saturation (i.e., 1 to 8). All target waypoints were spatially joined to their respective buffer unions for saturation field assignment.

Operation data sets consisted of (1) area, (2) time, (3) targets, and (4) projectile consumption, which were used to calculate target density (targets ha^{-1}), search efficiency (min ha^{-1}), and herbicide use rate (g ae ha^{-1}). The data and calculations were each assigned to three separate subcategories:

1. momentary intervention assignment (momentary)—an independent intervention data set with no saturation field assignments, generating gross area and operation performance values of the moment;
2. cumulative intervention assignment (cumulative)—a compilation of sequential data sets scaled by the number of interventions with progressive assignments made to a changing saturation field mosaic, generating net area and compounded operation performance values; and
3. historic intervention assignment (historic)—all sequential data sets were retroactively assigned to the final saturation field mosaic, generating gross area and operation performance values for each momentary operation in retrospect.

Momentary data sets were used to calibrate search efficiency and herbicide use rate corresponding to encountered target densities from independent flight segments (n = 103) contributing to the sequential interventions (n = 48).

Cumulative data sets were used to calculate weighted mean saturation ($\overline{Csat_n}$) from the net area field mosaic with the sum of each (ith) saturation level adjusted by the respective proportion of assignments, divided by the total field assignments within the entire mosaic (Equation 2). In this study, x_i includes either area or target assignments with the highest (ith) level of saturation equivalent to (n) interventions.

$$\overline{Csat_n} = \sum_{i=1}^{n} (ix_i) \Big/ \sum x_i \quad [2]$$

Cumulative target densities (Ctd_n) were adjusted by dividing the compounded values with their respective number (n) of contributing interventions (Equation 3). The influence of sequential interventions on the adjusted target density was fit with an exponential decay function for each patch (Equation 4).

$$Ctd_n = (Ca_n / Ct_n)/n \quad [3]$$

$$f(x) = y_o e^{-\lambda n} \quad [4]$$

Momentary and historic target densities only represent outcomes of the moment, which is dependent on the area searched and targets detected within that intervention. Cumulative target densities, on the other hand, account for targets dispatched in all previous interventions for the entire net area, providing a more spatially accurate presentation of progress.

Detection efficacy (de), as described by Leary et al. (2013), is the ratio of targets (x) recorded between sequential interventions (n) spatially assigned to the same saturation fields (Equation 5).

$$de = x_n / x_n + x_{n+1} \quad [5]$$

Retroactive proportions of cumulative target and net area totals ($Cprop_x$) of each intervention were calculated from the final total (Equation 6).

$$Cprop_x = Cx_n / Cx_{final} \quad [6]$$

Cumulative target proportions were plotted against their corresponding coverage (c), which was calculated as the weighted mean net area saturation (Equation 4) multiplied by the cumulative net area proportion for each intervention (Equation 7).

$$c = \overline{Csat_n} \times Cprop_n \quad [7]$$

Coverage of the last interventions ($Cprop_x$ = 1) of each patch were equal to the highest weighted mean saturation levels. These values were plotted with search theory concepts postulating probabilities of detection (P_d) for a random search operation (Equation 1) (Koopman 1946, 1980) and also a theoretically perfect "definite range" sensor (Equation 8) where P_d is proportional up to complete coverage (c = 1), resulting in perfect detection that cannot be exceeded with added coverage:

$$\lim_{c \to 1} (P_d \propto c) \quad [8]$$

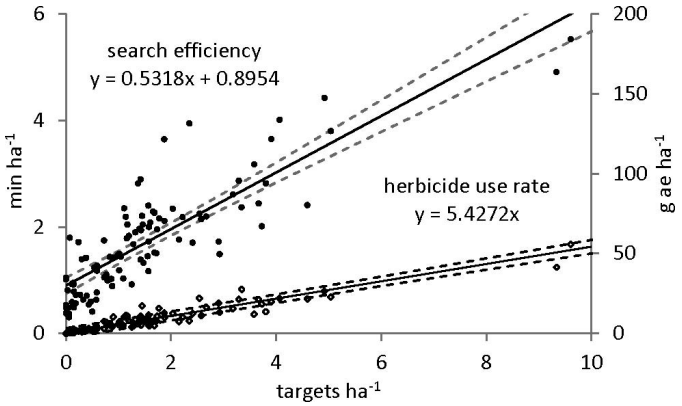

Figure 2. A scatter plot with best-fit lines and 95% confidence intervals (dashed lines) for surveillance efficiency (dark circles; min ha^{-1}; P < 0.001; R^2 = 0.78) and herbicide use rate (open diamonds; g ae ha^{-1}; P < 0.001; R^2 = 0.91) corresponding to encountered target densities (targets ha^{-1}) derived from momentary operation flight segments (n = 103).

Polynomial linear and two-parameter exponential decay functions were used to fit momentary and cumulative sequential data plots, respectively, using SigmaPlot® (version 12.0, (Systat Software, Inc., San Jose CA).

Results

In a 14-mo period, starting in February 2012, a total of 48 interventions were administered to the seven patches, covering 1138.1 net ha and dispatching 4,029 targets (Table 1). In total, 5,116.4 min of operation flight time (ca. 85.3 h) and 115,565 projectiles were utilized to accomplish these results. HAWI was the last patch on which the accelerated strategy was initiated and it was administered only four interventions, whereas WALU, NULU, and KANE were administered twice as many. Except for WAHI, all patch net areas were > 100 ha, with KANE being the largest at 214.9 ha, which also recorded the highest number of dispatched targets (i.e., 1,096 targets). Effective applications of previous interventions were visually confirmed even for the shortest time interval (i.e. 18 d). Only 88 survivors were retreated, indicating 98% efficacy with the HBT platform (data not shown).

Linear fits for search efficiency and herbicide use rate were highly significant when plotted against target densities

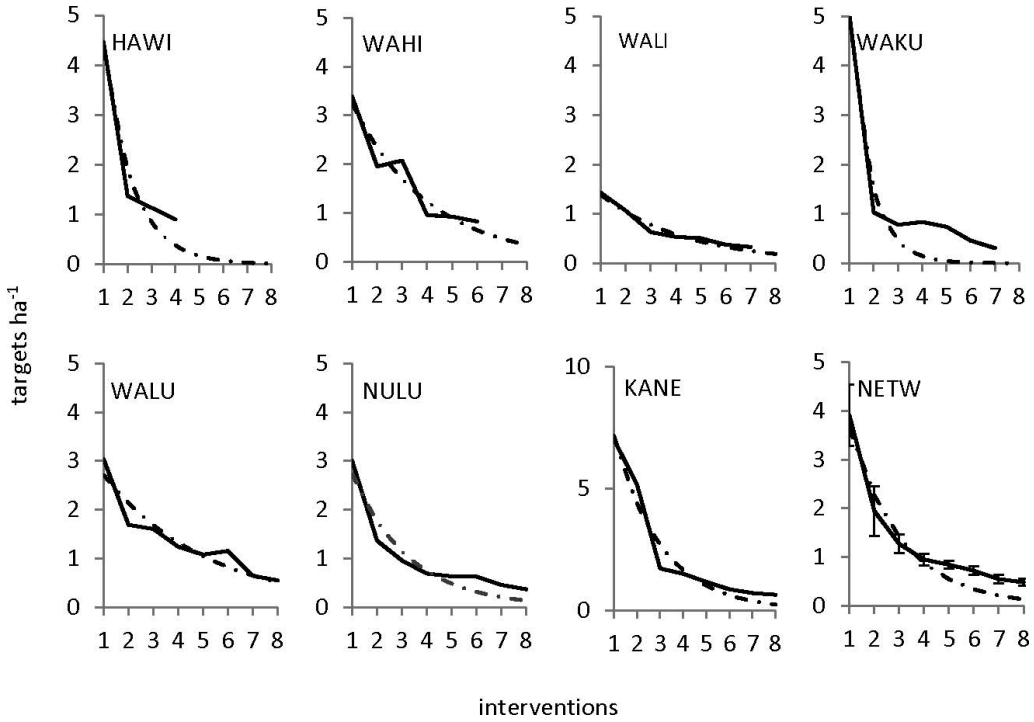

Figure 3. Adjusted cumulative target densities (targets ha^{-1}; solid black lines) of each patch and the entire network (± SE; $n = 7$ for one to four interventions; $n = 6$ for five or six interventions; $n = 5$ for seven interventions and $n = 3$ for eight interventions) with best-fit exponential decay functions (black dot-dash lines; $P < 0.05$; $R^2 > 0.88$). Notice KANE with a larger target density scale on the *y*-axis.

encountered ($P < 0.001$; $n = 103$) (Fig. 2). Search efficiency was measured at 0.90 min ha^{-1}, dispatch time at 0.53 min $target^{-1}$, and herbicide dose was estimated at 32 projectiles $target^{-1}$. All herbicide use rates were < 1% of the maximum allowable rate (i.e. 672.0 g ae ha^{-1}). The high coefficients of determination illustrated a strong dependence to target density, and validated platform consistency with previously published results (Leary et al. 2013), despite the use of multiple pilot/applicator teams across seven different sites.

All patches displayed reductions in cumulative target densities (adjusted by the number of interventions), following their respective intervention sequences. All reductions were significantly fit to exponential decay functions ($P < 0.05$; $R^2 > 0.88$; coefficient of variation for the root mean square residuals between observed and fitted values < 0.393) despite the variability of initial target densities (1.4 to 7.0 target ha^{-1}) and intervention sequences (four to eight interventions) (Figure 3; Table 2). Two general observations were made: (1) the sharpest reductions in target density occurred within the first three interventions and (2) targets were dispatched in every operation. Similar reductions were also observed for momentary target density sequences, but with greater peak deviations from the best-fit decay functions (data not shown). Cumulative target densities are comprehensive values of the entire patch, with reduction observed when target density of the last intervention was less than the net value of all previous interventions. These decay functions were influenced by a diminishing number of targets recorded in the latter interventions, with the curve asymptotically approaching zero, which will continue even beyond the point of eventually recording momentary undetectable levels.

Mean momentary search efficiency and herbicide use rate were reduced with each sequential intervention, corresponding to lower target densities encountered (Figure 4). Search efficiency is optimized when no targets are detected (Leary et al. 2013). As target density reduced to < 1 target ha^{-1} (i.e., operations 7 and 8), mean search efficiency was approximate to the calculated *y*-intercept coefficient (see Figure 2), suggesting some discrepancy between these independent derivations. Herbicide use rate showed a similar reduction trend with the final mean value equivalent to 0.06% of the maximum allowable use rate. Thus, the efficacy of previous interventions contributed to improved performance efficiencies for subsequent interventions on these accelerated schedules.

Mean net area increased with every sequential operation (Figure 5). This is due in part to improved search efficiencies making operational flight time available for expanding area coverage (see Figure 4). Net area expansion influenced the exponential decay of the cumulative target densities, with fewer targets being dispatched in these surrounding areas.

Table 2. Parameters of the exponential decay function estimated for each patch.

Patch	TD_i[a,b] (targets ha^{-1})	λ[c]	P[d]	R^2	$CV_{(RMSR)}$	TD_f (targets ha^{-1})
HAWI	4.5	0.808	0.041	0.92	0.222	0.9
WAHI	3.4	0.322	0.003	0.91	0.165	0.8
WAKU	5.0	1.170	0.001	0.89	0.392	0.3
WALI	1.4	0.286	< 0.001	0.96	0.113	0.3
WALU	3.0	0.239	< 0.001	0.90	0.176	0.5
NULU	3.0	0.434	0.003	0.90	0.259	0.4
KANE	7.0	0.488	< 0.001	0.95	0.215	0.6
NETW[e]	3.9 ± 0.2	0.476	< 0.001	0.94	0.229	0.5 ± 0.1

[a] Abbreviations: TD, target density; $CV_{(RMSR)}$, coefficient of variation for the root mean square residuals between observed and fitted values; TD_f, final adjusted cumulative target densities; HAWI, Hanawi; WAHI, Waihiumalu; WAKU, Waiakuna Pond; WALI, Wailua iki; WALU, Wailua nui, NULU, Nuuailua; KANE, Keanae Wall; NETW, network.

[b] Initial adjusted cumulative target densities.

[c] Decay function exponent.

[d] P value for nonlinear regression.

[e] The mean TD_{i-f} ± SE of the entire patch network with the other calculations based the best-fit exponential decay curve.

Mean saturation for net area and target assignments increased with each sequential operation (Figure 6). The positive trends are an indication of the strategy's adaptive quality for revisiting known target locations. The rate of cumulative target saturation advanced nearly three times faster than net area saturation as determined by slope coefficients of best-fit linear models ($P < 0.001$, $R^2 > 0.98$; data not shown). Cumulative target saturation was influenced by progressive reassignment of former dispatched targets to their next level of saturation, along with continued detection of new targets in these same saturated fields. Net area saturation was influenced by the same adaptive paradigm of saturation reassignment, and was also counter influenced by net area expansions with new unsaturated fields where less targets were detected, as stated above (see Figure 4).

Distinct differences in saturation field assignments were observed between final net areas and historic target points were distinct for all patches (Figures 7 and 8). Net area assignments were overrepresented by the lowest saturation level, whereas historic target assignments were overrepresented by the highest saturation levels. For instance, the expanded area for the entire patch network was almost six times larger than the highest saturation levels of each patch combined. By comparison, historic target assignments in

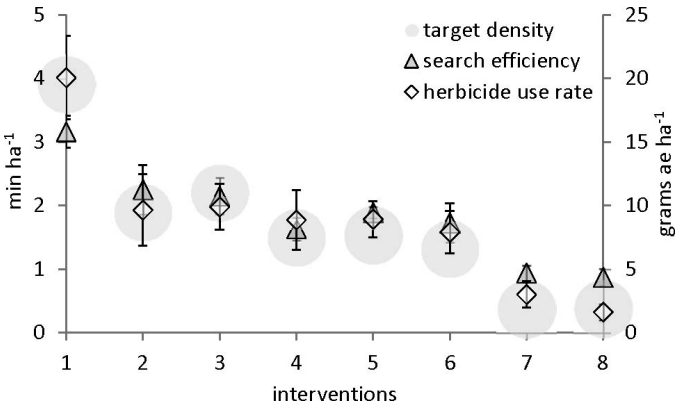

Figure 4. Mean search efficiencies (dark triangle) and herbicide use rates (light diamond) derived from momentary interventions (± SE; $n = 7$ for one to four interventions; $n = 6$ for five or six interventions; $n = 5$ for seven interventions and $n = 3$ for eight interventions) with mean momentary target density serving as a backdrop for each sequential operation. Backdrops appear oversized and transparent for the sole purpose of referencing target densities to the intervention performance values in focus and do not constitute any variance or deviation of the mean.

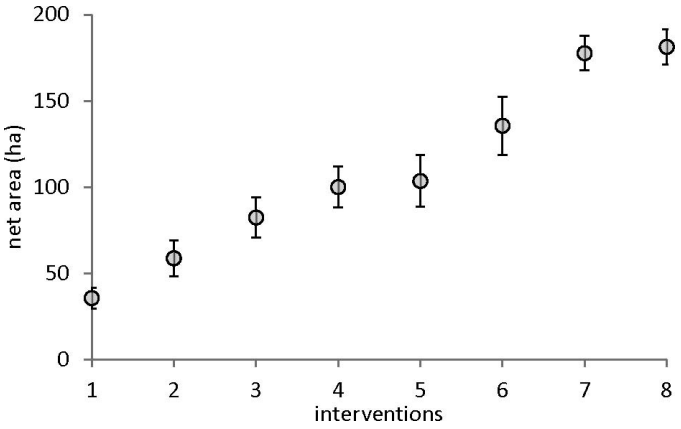

Figure 5. Mean cumulative net areas of sequential interventions (± SE; $n = 7$ for one to four interventions; $n = 6$ for five or six interventions; $n = 5$ for seven interventions and $n = 3$ for eight interventions).

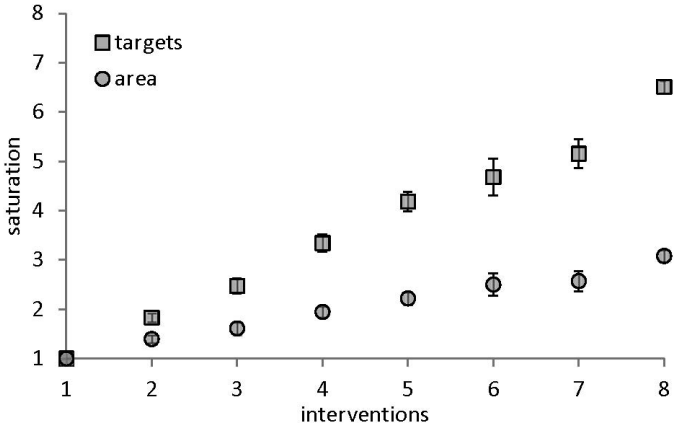

Figure 6. Weighted mean saturation for cumulative target (dark squares) and net area (light circles) field mosaic assignments (± SE; $n = 7$ for one to four interventions; $n = 6$ for five or six interventions; $n = 5$ for seven interventions and $n = 3$ for eight interventions).

the highest saturation levels were 20 times greater than total representation in the lowest saturation level. In practical terms, this highlights the basic elements of an adaptive surveillance process for delimiting satellite populations by continuing to revisit known target locations as long as new targets are being detected, while also progressively expanding surveillance coverage into new territories where finding targets is a more anomalous occasion.

As an example, Figure 9 shows the spatial dynamics of the sequential interventions imposed on the KANE patch. Similar to all of the other patches, this adaptive sequence depicts (1) target reduction and (2) net area expansion and increased complexity of the saturation field mosaic. Also, target detections are recorded throughout the net area, but with a majority of targets consistently recorded in the highest-saturation fields.

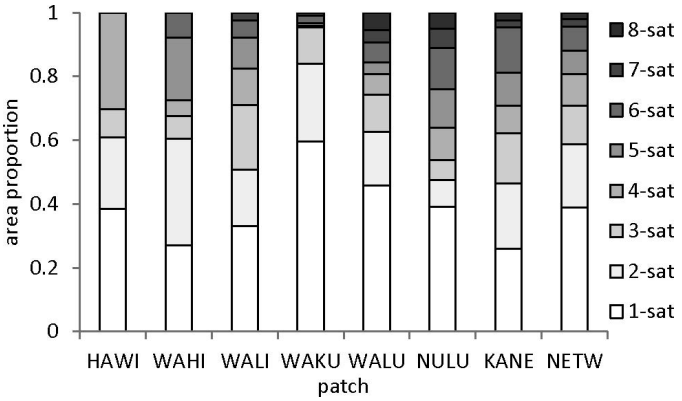

Figure 7. Proportion of the final cumulative net area assignments to the saturation field mosaic of each patch. NETW represents the proportion of the total assignments for all seven patches.

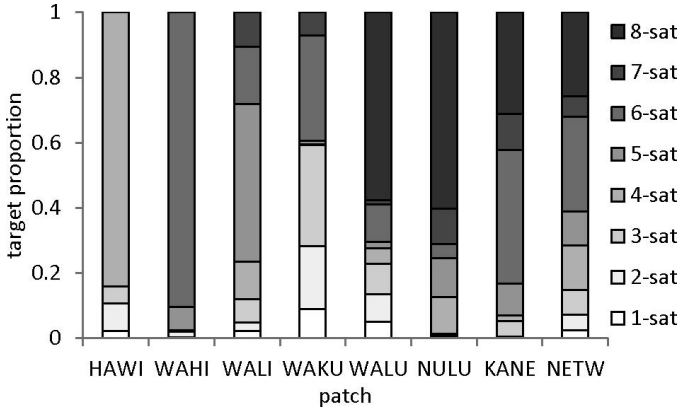

Figure 8. Proportion of historical target assignments to the final saturation field mosaic of each patch. NETW represents the proportion of the total assignments for all seven patches.

Mean detection efficacy of all interventions ranged from 0.56 to 0.76 (Figure 10). The phenomenon of imperfect detection is likely the artifact of two conditions: (1) false negative (type II) error with a failure to detect or (2) biological recruitment of target individuals achieving stature that exceeds the threshold of detectability. Mean detection efficacy of the entire patch network was 0.62 ± 0.3, which is conspicuously close to the probability of detection (P_d) of a random search operation (i.e. 0.63) where coverage (c) equals 1 (Koopman 1946, 1980). Detection efficacy, as measured in this study, is an empirical value between sequential interventions where coverage of the overlapped field is equal to 1. Cumulative target proportions ($n = 41$) plotted against their corresponding coverage values also fit closely with the exponential detection function for a random search operation (Figure 11).

Discussion

Miconia has been naturalizing in the EMW for over 40 yr, with the extant of the invasion approaching 20,000 ha, making containment the current management goal (Duncan and Leary 2013). Over the last two decades, fluctuations in funding have guided management decisions. Efforts to reduce high-density infestations have been prioritized in well-funded years, although more often the priority is to focus efforts on reducing low-density nascent foci (Taylor and Hastings 2004). The HBT platform is specifically designed for treating individual weed targets, and is ideal for administering interventions to low-density patch populations. Adoption of this technology has invigorated the miconia containment strategy with accelerated interventions measurably reducing the nascent patch network within a short period of time. In the 14-mo period reported here, operations increased by 33% over the average number of operations (per 14 mo) conducted for

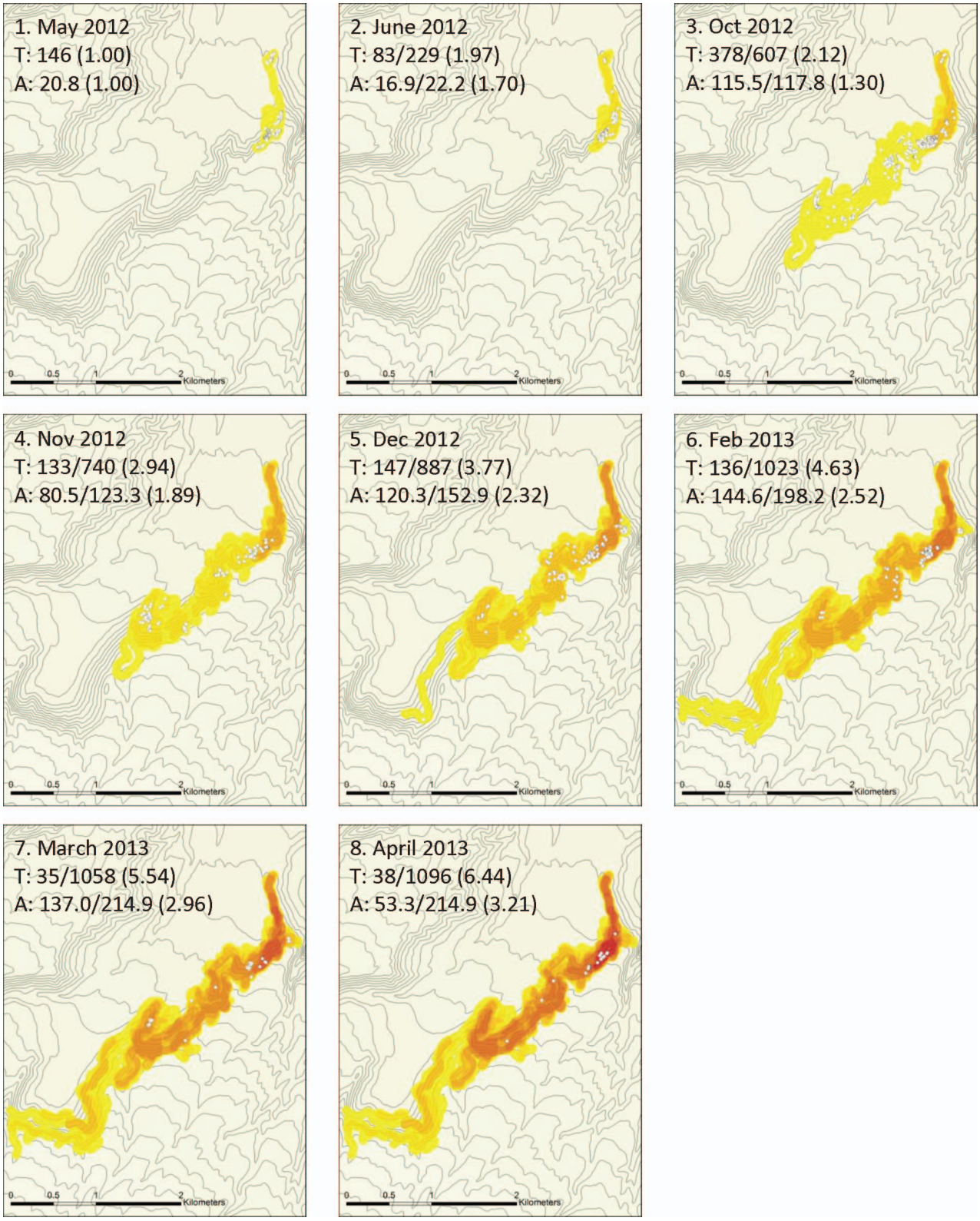

Figure 9. Intervention sequence (1 to 8) for KANE patch showing targets dispatched (white circles) and the net area field mosaic with increasing levels of saturation (yellow-to-red). Targets (T) and area (A) are presented (momentary/cumulative) along with weighted mean saturation levels shown in parentheses. 30-m contours displayed on the base map. (Color for this figure is available in the online version of this paper.)

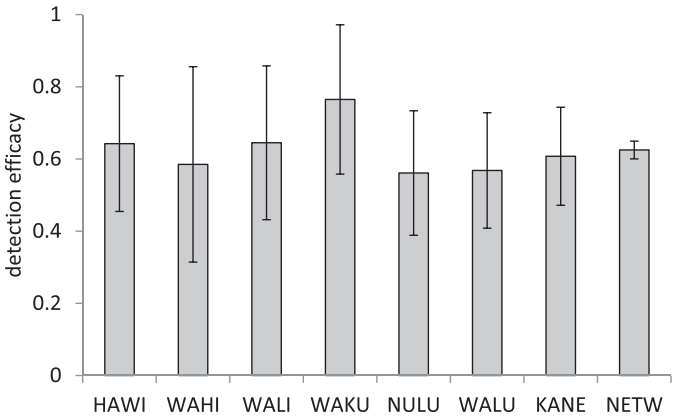

Figure 10. Mean detection efficacy (± SD; n = no. of interventions − 1; refer to Table 1) of each patch including the entire patch network (NETW; mean of all patches ± SE, $n = 7$).

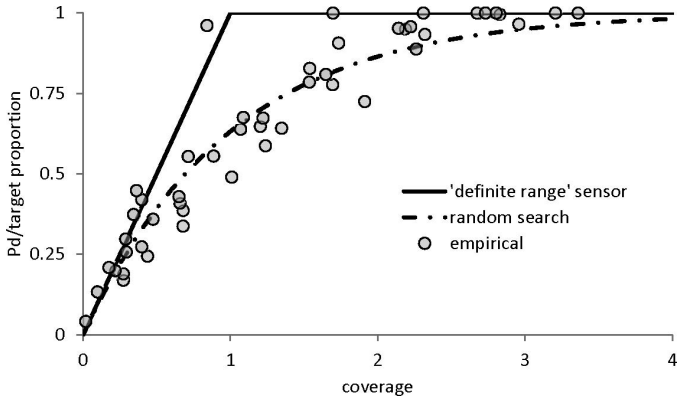

Figure 11. Sequential cumulative target proportions ($n = 48$) plotted against their respective weighted mean saturation values, along with P_d of a theoretical "definite range" sensor (solid black line; Equation 8) and a random search operation (black dot-dash; Equation 1) (Koopman 1946, 1980).

the entire patch network from 2005 to 2011. Consequently, the number of targets eliminated increased by 168% (Supplemental Table 1, http://dx.doi.org/10.1614/IPSM-D-13-00059.TS1). It is worth reiterating that these patch networks are in remote areas, accessible only to aerial operations. In these cases, the HBT platform improves target accessibility with capabilities in delivering an effective herbicide dose with horizontal trajectory and long range accuracy, relative to current aerial treatment options that must line up directly over the target (e.g., long line sprayer). We are also continuing to validate high treatment efficacy of HBT. In reference to the mortality factor, the HBT platform provides assurance that detectability is the limiting factor (Leary et al. 2013). This study shows how detectability can be improved by accelerating the intervention schedule. Eventually, future operations will begin recording momentary undetectable target levels with intermittent detection of recruitment events leading to exhaustion of a latent seed bank.

The entire spatial distribution of a weed invasion must be properly delimited to ensure effective containment (Panetta and Lawes 2005). The surveillance/intervention approach used in this study shares some of the qualities for a delimiting process described by Leung et al. (2010), in which they highlight the (1) approach, (2) decline, and (3) delimitation of a patch as an inside-out tactic for determining an effective containment boundary. All of the patches in this study are in the "decline" stage, where the least number of targets are assigned to the lowest-saturation fields (Figure 8), which also tend to be spatially located on the peripheries of the respective net area mosaics (see Figure 9). This strategy will not proceed to the "delimit" stage until all targets have been assigned to multi-saturated fields and net area has expanded beyond the most distal target assignments.

The detection efficacies recorded for these interventions fit the description of a random search operation (Cooper et al. 2003). A theoretically perfect search of a "definite range" sensor detects 100% of all targets with complete uniform coverage, making any further investment in search effort a waste of resources (Koopman 1946, 1980). However, any randomness in a search effort will reduce P_d (Cacho et al. 2006, 2007; Cooper et al. 2003; Frost 1999). In fact, for a random search operation, it would take three successive interventions with no detections recorded in order to assume a high probability of 0.98 that no targets are in the area. Only two of the seven patches have a final coverage > 3.0 in this study. However, targets continued to be recorded up to the last intervention, which strongly suggests the possibility of target recruitment taking place during the course of this study. This is further supported by a significant linear decline in detection efficacy from 18 to 182 d between interventions ($P < 0.039$, $R^2 = 0.127$; data not shown), suggesting a greater possibility of new recruitment with longer time intervals. With the combination of imperfect detection and active recruitment, future interventions that record undetectable levels should not serve as absolute confirmation of population extirpation. However, it does provide the opportunity to more accurately record intermittent detections as intrapatch recruitment (i.e., spatially assigned to high-saturation fields) or stochastic dispersal events (i.e., spatially assigned to low-saturation fields).

In a weed management scenario, randomness resulting in type II errors might include (1) physical stature of a plant target, (2) spatial arrangement of cohorts within the landscape, or (3) search capability (Cacho et al. 2004). Individual miconia targets can grow > 1 m in height in 1 yr, reaching a detectable threshold within that time period. Thus, what was undetectable in the previous interventions will eventually become detectable in subsequent interventions. These patch populations tend to be well hidden in topographic drainages and ravines as an understory to a complex forest canopy structure, creating impediments to clear sight lines. As a frugivore-dispersed

propagule, miconia targets have been commonly found hiding behind the trunks of canopy trees that have presumably served as bird defecation perches. The helicopter operations performed in these extreme three-dimensional spaces are also likely incurring randomness during the search effort. The operation flight lines are not perfectly spaced parallel tracks on a two-dimensional plane (as in ocean search and rescue), but instead are anisotropic to the terrestrial landscape with intent by the pilot to overlap the fields of view for each track with altimeter adjustments and visual cues in the landscape. The exponential detection function (P_d) is solely dependent on the amount of search effort applied uniformly to an area, regardless of whether it is applied all at once or incrementally (Koopman, 1946, 1980). Admittedly, the adaptive approach to saturating coverage in known target locations is not a uniform process, yet net coverage derived from the weighted mean saturation values still show good correspondence to the P_d of a random search operation. Furthermore, if recruitment and growth to detectable target size is actively occurring, total search effort applied to a single intervention would likely be ineffective. The early development of herbicide symptoms on miconia was critical to distinguishing new (untreated) targets in subsequent interventions. This feature alone allowed for the acceleration of intervention deployments, leading to an increased probability of target detection in rapid succession.

In this study, there are three potential outcomes to an intervention:

1. expansion—initial area coverage naive to any target encounters, which could be the first operation or a subsequent, sequential operation expanding beyond known target locations;
2. saturation—sequential interventions covering known locations with measurable reductions in target detection; or
3. confirmation—the final sequence of interventions monitoring momentary undetectable target levels with the likelihood of intermittent detections characterized as recruitment events, particularly in known target locations.

As the net area surveyed for each patch continues to expand, major portions of the network will amalgamate into a contiguous and complex saturation field mosaic. Continuing to build on this intelligence will provide clear depictions of active target locations surrounded by confirmed protected areas. The fit of empirical target values to exponential decay and detection functions prove that this accelerated intervention strategy is outpacing the biological recruitment of this highly invasive species. As progress continues, new strategies will lead to a deceleration of interventions and a refinement of coverage, optimizing future operations within the framework of an efficient, long-term containment strategy.

Acknowledgments

This project was funded in parts by U.S. Department of Agriculture (USDA) Forest Service, Special Technology Development Program Award R5-2012-01 through a collaboration with the Hawaii Department of Land and Natural Resources Forest Health Program, the USDA Hatch Act Formula Grant project 112H, and Maui County Offices of Economic Development and Department of Water Supply. The USDA, the State of Hawaii, and the County of Maui are equal opportunity providers and employers. We would also like to give our special appreciation to Mr. Chuck Chimera for his editorial improvements and local expertise. The authors claim no conflict of interest in this report.

Literature Cited

Anonymous (2000) Endangered and Threatened Wildlife and Plants; Determinations of Prudency and Designations of Critical Habitat for Plant Species from the Islands of Maui and Kahoolawe, Hawaii. U.S. Fish and Wildlife Service, 65 FR 79192. CFR: 50 CFR 17. RIN: 1018-AH70, Doc no. 00-31078, Pp 79192–79275

Anonymous (2007) Intelligence, Surveillance and Reconnaissance Operations. Air Force Doctrine Document 2–9. 66 p

Baxter PWJ, Possingham HP (2011) Optimizing search strategies for invasive pests: learn before you leap. J Appl Ecol 48:86–95

Cacho OJ, Hester S, Spring D (2007) Applying search theory to determine the feasibility of eradicating an invasive population in natural environments. Aust J Agric Res Econ 51:425–433

Cacho O, Spring D, Pheloung P, Hester S (2004) Weed Search and Control: Theory and Application. Agricultural and Resource Economics, University of New England, Armidale NSW 2351.Working paper No. 2004-11. 17 p

Cacho OJ, Spring D, Pheloung P, Hester S (2006) Evaluating the feasibility of eradicating an invasion. Biol Invasions 8:903–917

Chimera CG, Medeiros AC, Loope LL, Hobdy RH (2000) Status of management and control efforts for the invasive alien tree *Miconia calvescens* DC. (Melastomataceae) in Hana, East Maui. Honolulu, HI: University of. Hawaii, Pacific Coop Studies Unit, Tech Rep 128. 58 p

Cooper DC, Frost JR, Robe RQ (2003) Compatibility of land SAR procedures with search theory. Department of Homeland Security, U.S. Coast Guard Operations Technical Rep DTCG32-02-F-000032. 177 p

Cousens R, Mortimer M (1995) Dynamics of Weed Populations. New York: Cambridge University Press. 348 p

Denslow JS (2003) Weeds in paradise: thoughts on the invasibility of tropical islands. Ann Mo Bot Gard 90:119–127

Duncan C, Leary JK (2013) Protecting Paradise through Partnerships. http://techlinenews.com/articles/2013/3/13/protecting-paradise-through-partnerships. Accessed June 10, 2013

Fox JC, Buckley YM, Panetta FD, Bourgoin J, Pullar D (2009) Surveillance protocols for management of invasive plants: modelling Chilean needle grass (*Nassella neesiana*) in Australia. Divers Distrib 15:577–589

Frost JR (1999) Principles of search theory, part II: effort, coverage, and POD. Response 17:8–15

Giambelluca TW, Chen Q, Frazier AG, Price JP, Chen YL, Chu PS, Eischeid JK, Delparte DM (2013) Online rainfall atlas of Hawai'i. Bull Am Meterol Soc 94:313–316

Gilbert B, Levine JM (2013) Plant invasions and extinction debts. Proc Natl Acad Sci U S A 110:1744–1749

Hardesty BD, Metcalfe SS, Westcott DA (2011) Persistence and spread in a new landscape: dispersal ecology and genetics of Miconia invasions in Australia. Acta Oecol 37:657–665

Hester SM, Brooks SJ, Cacho OJ, Panetta FD (2010) Applying a simulation model to the management of an infestation of miconia

(*Miconia calvescens* DC.) in the wet tropics of Australia. Weed Res 50: 269–279
Jacobson MK (2005) Fundamentals of Atmospheric Modeling. 2nd edn. New York: Cambridge University Press. 828 p
Koopman BO (1946) Search and Screening. OEG Report No. 56, The Summary Reports Group of the Columbia University Division of War Research). Alexandria, Virginia: Center for Naval Analyses. 172 p
Koopman BO (1980) Search and Screening: General Principles with Historical Applications. Revised. New York: Pergamon. 400 p
Lawes RA, McAllister RRJ (2006) Using networks to understand source and sink relationships to manage weeds in riparian zone. Pages 466–469 *in* Preston C, Watts JH, Crossman ND, eds. Proceedings of the 15th Australian Weed Conference: Managing Weeds in a Changing Climate. Adelaide, Australia: Weed Management Society of South Australia
Leary JK, Gooding J, Chapman J, Radford A, Mahnken B, Cox LJ (2013) Calibration of an herbicide ballistic technology (HBT) helicopter platform targeting *Miconia calvescens* DC. in Hawaii. Invasive Plant Sci Manag 6:292–303
Leung B, Cacho OJ, Spring D (2010) Searching for non-indigenous species: rapidly delimiting the invasion boundary. Divers Distrib 16: 451–460
Lodge DM, Williams SL, MacIsaac H, Hayes K, Leung B, Reichard S, Mack RN, Moyle PB, Smith M, Andow DA, Carlton JT, McMichael A (2006) Biological invasions: recommendations for U.S. policy and management. Ecol Appl 16:2035–2054
Mack RN, Simberloff D. Lonsdale WM, Evans HC, Clout M, Bazzaz FA (2000) Biotic invasions: causes, epidemiology, global consequences and control. Ecol Appl 10 689–710
Medeiros AC, Loope LL, Conant P, McElvaney S (1997) Status, ecology and management of the invasive plant *Miconia calvescens* DC. (Melastomataceae) in the Hawaiian Islands. Bishop Mus Occas Pap 48:23–36
Meyer J-Y (1996) Status of *Miconia calvescens* (Melastomataceae), a dominant invasive tree in the Society Islands (French Polynesia). Pac Sci 50:66–76
Meyer J-Y (1998) Observations on the reproductive biology of *Miconia calvescens* DC. (Melastomataceae), an alien invasive tree on the island of Tahiti (South Pacific Ocean). Biotropica 30:609–624
Meyer J-Y, Florence J (1996) Tahiti's native flora endangered by the invasion of *Miconia calvescens* DC. (Melastomataceae). J Biogeog 23: 775–781
Meyer J-Y, Loope LL, Goarant AC (2011) Strategy to control the invasive alien tree *Miconia calvescens* in Pacific islands: eradication, containment or something else? Pages 91–96 *in* Veitch CR, Clout MN, Towns DR, eds. Island Invasives: Eradication and Management. Gland, Switzerland: International Union for Conservation of Nature
Moody ME, Mack RN (1988) Controlling the spread of plant invasions: the importance of nascent foci. J Appl Ecol 25:1009–1021
Moore JL, Hauser CE, Bear JL, Williams NSG, McCarthy MA (2011) Estimating detection-effort curves for plants using search experiments. Ecol Appl 21:601–607
Murphy HT, Hardesty BD, Fletcher CS, Metcalfe DJ, Westcott DA, Brooks SJ (2008) Predicting dispersal and recruitment of *Miconia calvescens* (Melastomataceae) in Australian tropical rainforests. Biol Invasions 10:925–936
Panetta FD, Lawes R (2005) Evaluation of weed eradication programs: the delimitation of extent. Divers Distrib 11:435–442
Pouteau R, Meyer J-Y, Stoll B (2011) A SVM-based model for predicting the distribution of the invasive tree *Miconia calvescens* in tropical rainforests. Ecol Model 222:2631–2641
Regan TJ, Chades I, Possingham HP (2011) Optimally managing under imperfect detection: a method for plant invasions. J Appl Ecol 48: 76–85
Reaser JK, Meyerson LA, Cronk Q, DePoorter M, Eldrege LG, Green E, Kairo M, Latasi P, Mack RN, Mauremootoo J, O'Dowd D, Orapa W, Sastroutomo S, Saunders A, Shine C, Thrainsson S, Vaiutu L (2007) Ecological and socioeconomic impacts of invasive alien species in island ecosystems. Environ Conserv 34:98–111
Rejmánek M, Pitcairn MJ (2002) When is eradication of exotic pest plants a realistic goal? Turning the tide: the eradication of island invasives. Pages 249–253 *in* Veitch CR, Clout MN, Towns DR, eds. Island Invasives: Eradication and Management. Gland, Switzerland: International Union for Conservation of Nature
Rew LJ, Maxwell BD, Dougher FL, Aspinall R (2006) Searching for a needle in a haystack: evaluating survey methods for non-indigenous plant species. Biol Invasions 8:523–539
Richardson DM, Allsopp N, D'Antonio C, Milton SJ, Rejmanek M (2000) Plant invasions—the role of mutualisms. Biol Rev 75:65–93
Spotswood EN, Meyer J-Y, Bartolome JW (2013) Preference for an invasive fruit trumps fruit abundance in selection by an introduced bird in the Society Islands, French Polynesia. Biol Invasions DOI 10.1007/s10530-013-0441-z
Taylor CM, Hastings A (2004) Finding optimal control strategies for invasive species: a density-structured model for *Spartina alterniflora*. J Appl Ecol 41:1049–1057
Thompson SK (2002) Sampling. 2nd edn. New York: J Wiley. 400 p
Wagner WL, Herbst DR, Sohmer SH (1999) Manual of the Flowering Plants of Hawaii. Revised edn. Honolulu: University of Hawaii Press/ Bishop Museum Press
[WRCC] Western Region Climate Center. http://www.wrcc.dri.edu. Accessed June 10, 2013

Received August 2, 2013, and approved November 18, 2013.

Calibration of an Herbicide Ballistic Technology (HBT) Helicopter Platform Targeting *Miconia calvescens* in Hawaii

James J. K. Leary, Jeremy Gooding, John Chapman, Adam Radford, Brooke Mahnken, and Linda J. Cox*

Miconia (*Miconia calvescens* DC.) is a tropical tree species from South and Central America that is a highly invasive colonizer of Hawaii's forested watersheds. Elimination of satellite populations is critical to an effective containment strategy, but extreme topography limits accessibility to remote populations by helicopter operations only. Herbicide Ballistic Technology (HBT) is a novel weed control tool designed to pneumatically deliver encapsulated herbicide projectiles. It is capable of accurately treating miconia satellites within a 30 m range in either horizontal or vertical trajectories. Efficacy was examined for the encapsulated herbicide projectiles, each containing 199.4 mg ae triclopyr, when applied to miconia in 5-unit increments. Experimental calibrations of the HBT platform were recorded on a Hughes 500-D helicopter while conducting surveillance operations from November 2010 through October 2011 on the islands of Maui and Kauai. Search efficiency (min ha^{-1}; $n = 13$, $R^2 = 0.933$, $P < 0.001$) and target acquisition rate (plants hr^{-1}, $n = 13$, $R^2 = 0.926$, $P < 0.001$) displayed positive linear and logarithmic relationships, respectively, to plant target density. The search efficiency equation estimated target acquisition time at 25.1 sec and a minimum surveillance rate of 67.8 s ha^{-1} when no targets were detected. The maximum target acquisition rate for the HBT platform was estimated at 143 targets hr^{-1}. An average mortality factor of 0.542 was derived from the product of detection efficacy (0.560) and operational treatment efficacy (0.972) in overlapping buffer areas generated from repeated flight segments ($n = 5$). This population reduction value was used in simulation models to estimate the expected costs for one- and multi-year satellite population control strategies for qualifying options in cost optimization and risk aversion. This is a first report on the performance of an HBT helicopter platform demonstrating the capability for immediate, rapid-response control of new satellite plant detections, while conducting aerial surveillance of incipient miconia populations.

Nomenclature: Miconia, *Miconia calvescens* DC. MICA20.

Key words: Hawaii, Herbicide Ballistic Technology.

The loss of endemic biological diversity due to exotic plant invasions is particularly detrimental on isolated islands (Denslow 2003; Mack et al. 2000; Reaser et al. 2007). Either eradication or containment of the invasive species can serve as viable mitigation strategies depending on which option has the greatest potential for success (Panetta 2009; Panetta and Cacho 2012; Taylor and Hastings 2004; Wittenberg and Cock 2001). Regardless of the approach, detection and control must be effectively applied to the entire population, particularly with the most isolated satellites (Brooks et al. 2009; Cacho et al. 2006; Hulme 2006; Myers et al. 2000; Panetta 2009; Panetta and Lawes 2005). Archiving knowledge of the target species is also critical to determine the management approach and would include studies on the biology (e.g. growth and fecundity), ecology (i.e. propagule dispersal) and physiography (i.e. suitable habitat) of the target species (Chimera et al. 2000; Florence 1993; Hardesty et al. 2011; Kuefer et al. 2010; Pouteau et al. 2011). An effective species mitigation strategy combines (1) practical knowledge, (2) sustained resources and (3) proven actions that progress towards a measurable reduction of target density and contraction of the delimited invasion perimeter.

DOI: 10.1614/IPSM-D-12-00026.1

* First and sixth authors: Assistant Specialist and Specialist, Department of Natural Resources and Environmental Management, University of Hawaii at Manoa, PO Box 269, Kula, HI 96790; second author: Liaison, Pacific Islands Exotic Plant Management Team, National Park Service, PO Box 880896 Pukalani, HI 96788; third author: Operations Planner/Analyst, Kauai Invasive Species Committee, P.O. Box 1998, Lihue, HI 96766; fourth and fifth authors: Operations Manager and GIS Specialist, Maui Invasive Species Committee, P.O. Box 983 Makawao, HI 96768. Corresponding author's Email: leary@hawaii.edu

Management Implications

Herbicide Ballistic Technology (HBT) is a novel application technique designed to deliver encapsulated herbicide projectiles with long-range accuracy and precision. We report on the performance of an HBT platform providing immediate control of miconia (*Miconia calvescens* DC.) satellite plants, detected while conducting helicopter surveillance calibrations in Hawaii's remote watersheds. Flight calibrations (n = 13) generated efficiency parameters related to the functionality of the platform. Plant target density was a significant variable for determining search efficiency (min ha^{-1}), target acquisition rate (plants hr^{-1}) and herbicide use (g ae ha^{-1}). The product of detection efficacy and treatment efficacy estimated population mortality (i.e. reduction) as another operational parameter used in simulation models to project feasibility and expected cost of different population reduction strategies based on cost optimization and risk aversion. This research is critical to our technology transfer program that includes development of the standard operating procedure for safe use of the HBT platform, which has been approved by the Pacific Cooperative Studies Unit, University of Hawaii and approval by the Hawaii Department of Agriculture for a FIFRA Section 24c Special Local Needs registration for HBT-G4U200 with Garlon® 4 Ultra (EPA SLN Reg. No. HI-120001), with miconia listed as a target species.

Miconia (*Miconia calvescens* DC.) is a mid-story tree, 12 to 15 m tall, native to Central and South America. It has large, bicolored leaves that are up to 80 cm in length, which made this species desirable to botanical hobbyists and horticultural professionals. This led to purposeful introductions to other suitable habitats throughout the Pacific (Meyer 1996). It is currently listed as one of the 100 worst global invasive species (Lowe et al. 2000), is a class 1 weed in Queensland, Australia (Hardesty 2011) and a state noxious weed in Hawaii, USA (Medeiros et al. 1997). The miconia infestation in Tahiti has been well characterized. After its introduction in 1937, it became the dominant vegetation to over 65% of the forest in less than 60 yr (Florence 1993; Meyer 1996). High densities of this shallow rooted species are known to shade out the understory vegetation and further suspected to promote soil surface erosion, particularly on steeper terrain (Giambelluca et al. 2010; Medeiros et al. 1997; Meyer 1996).

Miconia is an autogamous species that reaches maturity in 4 to 5 yr. A single plant has immense fecundity, with the ability to produce millions of propagules in a single reproductive cycle (Meyer 1998). Miconia produces a small, edible fruit, approximately 5.9 mm in diam (0.23 in) lending itself to frugivorous dispersal by a generalist avian population (Chimera et al. 2000). In Australia, both Hardesty et al. (2011) and Murphy et al. (2008) infer that 95% of dispersal events occur within 500 m, but with a maximum dispersal range that could go beyond 2000 m. The current recommendation is for maintaining radial management buffers that are at least 500 m, but preferably 1000 m (Hardesty et al. 2011). The most recent report from Tahiti has validated seed bank viability to be over 16 yr (Meyer et al. 2011). Thus, preventing satellite miconia populations from reaching maturity (i.e. elimination) is critical to mitigating the invasion.

Miconia was introduced to the Hawaiian Islands in 1961 (Medeiros et al. 1997). Thirty years later, the first management program was initiated on Maui and by 1996 management programs existed on the islands of Kauai, Oahu and Hawaii (Chimera et al. 2000). Population reduction (i.e. containment over eradication) was recently determined to be the optimal management policy for minimizing expected costs of control on Oahu, Maui and Hawaii. On Kauai, deferment of control was suggested due to the higher costs associated with searching in a much lower population density, (Burnett et al. 2007). Currently however, all islands, including Kauai, are operating under a more risk averse policy that implements surveillance and treatment operations focused on known incipient populations. This approach may have higher operational costs, but also presents greater opportunity to mitigate detrimental uncertainties regarding the extent of these invasions. Reduction of satellite populations can have a more mitigating effect on an invasion compared to control efforts in a higher density core infestation (Moody and Mack 1988). Search effort, particularly in remote natural settings, is a costly procedure, making plant detectability critical to effective containment (Cacho et al. 2007; Hester et al. 2010). Costs are further compounded when plant detection and treatment activities are performed in separate operations, which has often been the case for controlling miconia in Hawaii.

The herbicide active ingredient triclopyr is lethal to miconia in low doses as basal bark or foliar applications (Chimera et al. 2000; Medeiros et al. 1998). The aerial long line spray system currently used to treat miconia, was originally developed by the US Drug Enforcement Agency for marijuana (*Cannabis sativa* L.) control. A typical assembly consists of a 95 L tank (25 gal) mounted to the cargo hook of a Hughes 500-D helicopter and a tethered 30 m by 9 mm hose with a distal nozzle configuration for directed applications administered by the pilot. Most aerial operations are relegated to inaccessible locations and often require separate reconnaissance and treatment flights due to encumbrance of the long line sprayer (Burnett et al. 2007). This spray system relies on pilot dexterity to safely position the nozzle assembly directly overhead, and is typically limited to treating miconia in open tree canopy gaps and on shallow slopes. However, miconia is also able to reside on much steeper slopes up to 75° (Pouteau et al. 2011) and under impeding tree canopy (Meyer 1994), making it difficult or impossible for the long line sprayer to treat all targets. This limitation ultimately compromises the success

of an effective containment strategy (Myers et al. 2000, Panetta 2009).

Herbicide Ballistic Technology (HBT) is a novel herbicide delivery technique designed to discretely administer encapsulated herbicide aliquots through a pneumatic device to individual weed satellites with long-range accuracy. The effective treatment range is 30 m in either horizontal or downward vertical trajectories, while maintaining submeter accuracy. The high velocity impact of the projectile to the plant (ca. 50 m s^{-1}) creates a circular spatter pattern that is approximately 1 m^2, with our observation that a majority of the fluid is retained at the point of impact. This precision delivery platform is uniquely suited to treating satellite miconia residing on extreme topography or under tree canopy that would otherwise impede the long line sprayer.

The objectives of this study were to determine triclopyr efficacy when delivered as HBT projectiles to miconia and evaluate the utility of an HBT aerial platform in helicopter surveillance calibrations. The empirical performance measures were further utilized in model simulations with expected cost analyses to project effective containment strategies of incipient miconia populations.

Materials and Methods

The HBT Projectile. Batch processing of HBT projectiles was conducted by the Nelson Paint Company (EPA Est. No. 86199-MI-001) using standard in-house procedures for producing spherical soft gelatin capsules (17.3 mm dia.) with a 2.6 ml (0.09 fl. oz) liquid fill capacity. The HBT-TCP200 herbicide formulation is a simple bipartite blend of triclopyr (3,5,6,-trichloro-2-pyridinyloxyacetic acid, butoxyethyl ester; Garlon® 4 Ultra, EPA Reg. No. 62719-527, Dow® Agrosciences LLC Indianapolis, IN) diluted with a modified vegetable oil concoction of surfactants and coupling agents to produce a projectile unit with 199.4 mg ae. The HBT-IMZ31 herbicide formulation is imazapyr (2-[4,5-dihydro-4-methyl-4-(1-methylethyl)-5-oxo-1H-imidazol-2-yl]-3-pyridinecarboxylic acid; Arsenal® Powerline™, EPA Reg. No. 241-431, BASF® Corp., Triangle Park, NC) blended with the same adjuvant concoction to produce a projectile unit with 31.2 mg ae. HBT-TCP200 and HBT-IMZ31 formulations are comparable to 16% and 5% v/v, respectively.

Treatment Efficacy Validation. Two ground-based field trials were established in February 2010 to compare efficacy of the HBT-TCP200 and HBT-IMZ31 on miconia within the East Maui infestation (20°45′46″N, 156°01′17″W). The first experiment was conducted as a completely randomized design replicated three times with a 2 by 2 factorial treatment set comparing formulations (TCP200 vs. IMZ31) at two different application rates (5-unit vs. 10-unit). All experimental targets were juvenile miconia of relatively uniform size with a single leader stem between 3 to 5 m tall. Projectiles were administered at the lowest axial point from a 3 m range with a marker calibrated to discharge a projectile with a 100 m s^{-1} muzzle velocity. A second experiment compared the formulations as a 5-unit application rate targeting the base of the main leader stem approximately 30 cm from the soil surface. Visual confirmation of treatment lethality was conducted in September 2010 (227 DAT).

The Onboard HBT Platform. The three basic components of the onboard HBT platform include: (1) the HBT projectile inventory subdivided into pods (ca. 140 projectiles) serving as retention devices during transfer to the (2) electro-pneumatic application marker (BT® TM7™, Kee Action Sports LLC, Sewell, NJ) consisting of a microswitch-controlled solenoid actuating a 1380 kPa compressed air discharge for bolt-action propulsion of projectiles powered by (3) a regulated 1180 cm^3 aluminum reservoir tank pressurized up to 20,700 kPa. The marker was calibrated to launch projectiles through a 30 cm long, ceramic-coated, smooth bore barrel calibrated for a muzzle velocity of 100 m s^{-1} and a terminal range of just beyond 50 m. The tanks were connected to the marker via coiled high pressure remote line with quick connect coupler and sliding check valve for depressurized tank replacement. The complete onboard assembly consisted of forty pods (ca. 5,600 units), six tanks, and two markers. The platform was designed to match resource consumption (i.e. projectiles and compressed air) with operational flight time (ca. 100 min) and accommodate redundancy in the event of a minor component malfunction.

HBT Calibration Flight Segments and Site Locations. HBT platform calibrations were derived from flight segments of helicopter surveillance operations that were distinguished by date, time and site. Up to two segments were recorded from a single operation, although most operations had only one segment recorded. A total of thirteen calibration flight segments were recorded from October 2010 to November 2011 in three sites on the island of Maui: Wailua Nui (20°50′06″N, 156°08′06″W, three flight segments); Waiokamilo (20°50′03″N, 156°08′28″W, two sites with three flight segments each), and one site on the Island of Kauai: Opaekaa (22°04′50″N, 159°24′11″W, four flight segments).

In-flight HBT Calibration Protocols and Recorded Parameters. All calibrations were conducted onboard a Hughes 500-D helicopter with doors removed and a three-person crew configured with the applicator seated portside, posterior to the pilot and an additional spotter seated in the front, starboard side. All crewmembers were responsible for safety monitoring and miconia target detection. The target

Figure 1. An HBT operator positioned in the portside rear seat of a Hughes 500-D with a pneumatic device engaging two incipient miconia targets within effective range and a clear line of sight. Photo credit to Josh Atwood.

acquisition process between the pilot and the applicator was initiated by positive identification of the miconia target followed by the aircraft safely approaching to within a 30 m range and clear line of sight (PCSU 2011; see Figure 1). A target window was designated for the applicator to safely discharge projectiles within a 270° to 300°horizontal trajectory (i.e. 9 to 10 o'clock position) and a 200° to 270° vertical trajectory (i.e. landing skid to eye level). With the aircraft in a stationary position, the applicator obtained permission from the pilot to treat the target, discharged projectiles, recorded GPS waypoint and cued the pilot to continue with the operation. Detection from the helicopter was typically limited to miconia plants that were at least 1 m tall with fully expanded leaves (i.e. assumed to be at least 2nd-yr juveniles). All applications were administered as a 5-unit treatment to each visible axial point of the plant. Juvenile plants were supported by a single leader stem that could range from 1 to 4 m tall and typically had < 5 axial points, while larger (potentially mature) plants would display a spreading canopy with ≥ 5 axial points. All plant target waypoints and corresponding logs of the flight path were recorded with a GPS device (Foretrex® 301; Garmin® Olathe, KS) set to record geographical position, timestamp and velocity on 30-s intervals. Discrepancy between the recorded applicator location and the actual offset distance of the target should be noted. In most cases, closely approaching the target would have been hazardous or impractical and would also have confounded the time parameter of the calibration. All of the targets were located within 30 m of the recorded waypoint. Survivors of earlier treatments were also recorded for repeat calibrations and were identified as symptomatic targets with viable intact canopy and were administered retreatment to those living portions. Pod (ca. 140 projectiles) inventory consumption was recorded for each flight segment.

Platform Performance Calculations. Operational flight segments containing first and last recorded miconia targets were spliced from raw track logs by removing the ferry portions (determined by flight segments to and from the landing zone that exceeded 20 km hr^{-1}) using Mapsource® (version 6.12.4; Garmin® Olathe, KS). Net surveillance areas were calculated with a 50 m buffer on each side of the operational flight segments with overlapped portions dissolved using the buffer analysis tool in ArcGIS® (version 10.0; ESRI® Redlands, CA). The time interval between the timestamps of the start and end points were recorded. Plant target density was the product of targets acquired divided by the segment area, reported as targets ha^{-1}. Target acquisition rate was the product of the targets acquired divided by the segment time, reported as targets hr^{-1}. Search efficiency was the product of segment time divided by segment area, reported as min ha^{-1}. Detection efficacy was based on the assumption that all targets acquired in the subsequent overlapping segment were not detected in the previous segment and was calculated as the product of targets acquired in the previous segment divided by the composite of all targets acquired in the previous and subsequent segments. This is a conservative, but reasonable assumption that newly recorded miconia targets is more likely the result of crew detection errors in the previous operation than actual recruitment within the short time intervals between flight segments (i.e. 89 to 171 days). Operational treatment efficacy was the product of effectively treated targets divided by the total targets acquired. Effectively treated targets were deciphered by subtracting the number of survivors identified in the subsequent segment. Mortality factor as described by Cacho et al. (2007) is the product of the probability of detection multiplied by treatment efficacy. For this study, the mortality factor was empirically derived as the product of detection efficacy multiplied by operational treatment efficacy calculated from the repeated overlap areas. Target herbicide dose was calculated as the product of pod inventory consumption divided by the targets acquired in a flight segment. Similarly, herbicide use was calculated as the product of pod inventory consumption divided by the buffered surveillance area. Both projectile consumption parameters were reported in triclopyr acid equivalents based on a known quantity of each projectile (e.g. 199.4 mg ae).

Simulation Models and Expected Cost Analyses. Simulations of 1-yr population reduction strategies within buffered isotropic management areas (1 km radius = 314 ha) were performed to compare different management frequencies: (1) quarter-annual (four operations), (2) semi-annual (two operations) and (3) annual (one operation). The population density range was 0 to 315 targets. A

Table 1. Time and costs estimates ($USD) for helicopter operations.

	OFT[a]			Ferry[b]			Crew[c]		
	1/3 ops	2/3 ops	Full ops	1/3 ops	2/3 ops	Full ops	1/3 ops	2/3 ops	Full ops
1 heli	1.7 ($1,667)	3.3 ($3,300)	5.0 ($5,000)	1.1 ($1,133)	1.5 ($1,467)	1.8 ($1,800)	12.0 ($300)	19.5 ($488)	27.0 ($675)
2 heli	3.3 ($3,300)	6.7 ($6,700)	10.0 ($10,000)	2.3 ($2,267)	2.9 ($2,933)	3.6 ($3,600)	20.0 ($500)	32.5 ($813)	45.0 ($1,125)
3 heli	5.0 ($5,000)	10.0 ($10,000)	15.0 ($15,000)	3.4 ($3,400)	4.4 ($4,400)	5.4 ($5,400)	28.0 ($700)	45.5 ($1,138)	63.0 ($1,575)

[a] Operational flight time is the flight time dedicated to surveillance and target acquisition calculated from a fuel cycle of a Hughes 500D performing low-level hovering tactics, estimated at 120 total min minus 20 min round-trip ferry to and from the LZ. A full ops session accommodates 3 fuel cycles providing 5, 10, or 15 hours of operational flight time for 1, 2, or 3 helicopters, respectively. Utility helicopter flight services are $1000 hr^{-1}.

[b] Ferry time is non-operational flight time for round-trip transport of aircraft from the heliport (0.8 hrs rt) to the LZ and from the LZ to the management containment area (0.33 hrs rt). Each aircraft is committed to one round-trip heliport ferry and each ops fuel cycle is committed to one round-trip LZ ferry.

[c] Crew management consists of an operations manager plus two crew members for each aircraft. Logistical responsibilities include onboard HBT platform assembly, replenishment, refueling, flight following, navigation, surveillance and application. Wage is $25 person-$hr^{-1}$.

mortality factor of 0.542 (the average derived from the repeated flight segments) was imposed on each operation.The undetected targets were calculated from the subtracted product of the mortality factor, which served as the target population for the subsequent operations for quarter- and semi-annual strategies, respectively.

A structured matrix model developed for miconia by Hester et al. (2010) was adopted in this study to simulate strategies for eradicating incipient miconia populations. The model estimates annual population growth based on the probabilities of survival and succession of the (1) seed bank, (2) four distinct juvenile stages and (3) small and large mature plants generating positive-feedback by fruit production augmenting the seedbank. The model was modified using Meyer (1998) fecundity data where the average fruit per panicle was 208 with 195 seeds per fruit. For this model, a small mature plant only produced two panicles which is equivalent to 81,120 seed, while a large mature plant produced 50 panicles with 2,028,000 seed. The population vector (X_t) of this matrix model started with a seed bank of 668,075 propagules, 210 juvenile plants and 2 small mature plants (see Appendix 1). The average mortality factor of the HBT platform (0.542; see Table 5) was imposed on the matrix model targeting the juvenile stages 2 to 4 yr and adult stages, with the assumption that first-yr juveniles were undetectable. Population densities (mature/juvenile) were selected as management starting points that included: (1) 2/48, (2) 20/74 and (3) 209/1518 representing increasing levels of invasion identified along the growth model. The management frequencies were as described above and also included bi- and triennial strategies.

Expected cost estimations for both models were based on a helicopter flight cost of $1000 USD hr^{-1}, HBT projectile inventory consumption with a projectile price of $0.31 USD (Nelson Paint Company, personal communication) and crew costs of $25 USD person-$hr^{-1}$. Operational flight times were determined by solving for search efficiency (min ha^{-1}) dependent on plant target density and the lowest cost determined by the number of helicopters needed to accommodate that operation along with corresponding ferry times and crew labor (Table 1). Similarly, projectile inventory consumption was based on the equation that solves for herbicide dose, which was estimated to be 25 units per target. The 1-yr population reduction strategies were reported as basic cost estimates that would accommodate a manager submitting an annual budget request. The matrix model simulation calculated the net present values (NPV) of projected eradication timelines at a 6% discount rate applied to the annual cost of operations (Hester et al. 2010).

Regression analyses were performed using ordinary least squares to determine the effect of plant target density on empirically derived search efficiency, target acquisition rate and herbicide use ($n = 13$) and on expected cost estimates for the 1-yr population reduction strategies (SPSS. 2009. PASW Statistics 18, Release Version 18.0.0. SPSS, Inc., Chicago, IL).

Results and Discussion

The herbicide efficacy experiment determined HBT-TCP200 to be lethal with 5- and 10-unit treatments, applied either to canopy axial points or the base of the leader stem (Table 2). The HBT-IMZ31 treatments were not effective. The high velocity projectiles penetrated the thin epidermis of branches with a fraction of the herbicide creating a ''water soaked'' mark at the point of impact and

Table 2. Miconia survival after treatment with TCP200 and IMZ31 at the main stem axial points with 5- and 10-unit applications and basal treatments with 5-unit applications. Recorded 224 DAT.

	ri		rii		riii	
	Alive	Dead	Alive	Dead	Alive	Dead
Axial						
TCP-5		X		X		X
TCP-10		X		X		X
IMZ-5	X		X		X	
IMZ-10	X		X		X	
Basal						
TCP-5		X		X		X
IMZ-5	X		X		X	

the remaining portion scattered on to the leaf canopy, including the undersides. The option to effectively treat either the base or canopy of miconia is useful in an operational setting where a clear line of site at the base of the plant may not be available due to adjacent impeding vegetation. This herbicide efficacy experiment allowed us to proceed with further evaluating the utility of HBT in a helicopter platform using the HBT-TCP200 projectiles.

A total of thirteen HBT calibration flight segments were recorded with a single applicator, three different pilots and six spotters. Segment time intervals ranged from 13 to 92 min (Table 3). Segment lengths ranged from 508 to 16,276 m with corresponding buffer areas ranging from 4.9 to 121.4 ha. Target acquisitions ranged from 4 to 164 targets per segment and HBT projectile consumption from 2 to 27 pods per segment. Search efficiency, target acquisition rate and herbicide use were all correlated to plant target density, showing significant positive trends. Simple linear equations produced best fits for search efficiency (Figure 2; $R^2 = 0.933$; $P_{0.05} < 0.001$) and herbicide use (Figure 4; $R^2 = 0.966$; $P_{0.05} < 0.001$), while target acquisition rate was best fit with a logarithmic equation (Figure 3; $R^2 = 0.927$; $P_{0.05} < 0.001$).

According to the linear search efficiency equation (Figure 2), a helicopter surveillance operation was estimated to search one hectare in 1.13 min (ca. 68 s) where no targets were detected within the buffered area, while the slope coefficient estimated the complete target acquisition process to take 0.418 min (ca. 25 s) (Table 4). Thus, in areas with ≥ 3 targets ha^{-1}, the target acquisition time exceeded surveillance time. According to the logarithmic equation (Figure 3), the maximum target acquisition rate was projected to be 143 targets hr^{-1}, which was achieved at a density of 164 targets ha^{-1}, but exceeded 100 targets hr^{-1} when the density ≥ 8 targets ha^{-1}. This was represented in 5 of the 13 calibration flight segments (Figure 3). According to the linear herbicide use equation, each miconia plant received a mean herbicide dose of 4.79 g ae triclopyr (0.17 oz) which back calculates to an estimate of 24 projectiles per target. This would suggest an average plant size with 4 to 5 axial points assuming 100% accuracy of the designated 5-unit application rate. A majority of the

Table 3. Recorded HBT calibration flight segment data.

Island/Site	Date	T[a]	Lngt[a]	Area[b]	Targets	Pods[c]
		min	m	ha		
Maui						
Wailua Nui	11/10	61	1,896	7.8	134	27
	05/11	69	2,372	8.1	114	19
	08/11	64	3,125	15.6	71	15
Waiokamilo 1	04/11	60	1,402	8.2	140	22
	08/11	45	1,343	8.7	96	15
	08/11	92	3,849	19.8	164	23
Waiokamilo 2	05/11	26	756	6.3	33	5
	08/11	13	508	4.9	16	3
	08/11	13	571	5.1	19	3
Kauai						
Opaekaa	04/11	39	8,447	58.7	8	3
	06/11	73	9,048	70.0	5	2
	07/11	48	5,984	51.8	4	2
	10/11	69	16,276	121.4	7	2

[a] Flight segment time and length recorded from the start and end points of the track log.

[b] Area calculated from a 50 m buffer on both sides with overlap areas dissolved (see Materials and Methods).

[c] Estimated 140 projectiles per pod.

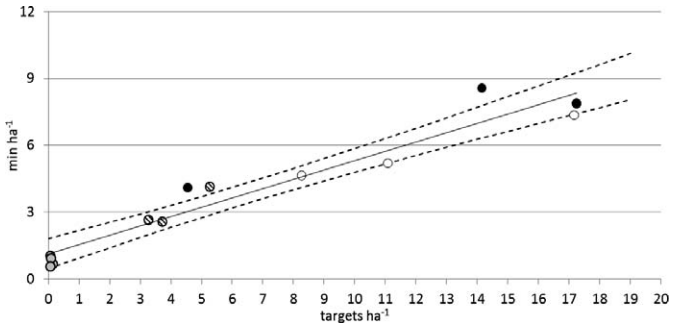

Figure 2. A scatter plot with best fit line (R^2= 0.927; P < 0.001) with 95% confidence interval (dash lines) of search efficiency (min ha^{-1}) versus target density (targets ha^{-1}) for HBT calibration flight segments (n = 13) conducted in Wailua nui (black), Waiokamilo 1 (white), Waiokamilo 2 (stripe) and Opaekaa (grey) from November 2010 to October 2011. See Table 4 for regression coefficients.

targets had 3 to 4 axial points and the accuracy of the application was not measured during the calibrations, but it was less than 100%. Furthermore, an axial point may have received > 5 units, but not more than 10 units. In comparison to other registered triclopyr products, the highest use rate of HBT-TCP200 was 1.09% of the maximum allowable rate of 8.96 kg ae ha^{-1}(8 lbs ae $acre^{-1}$) while the remaining twelve calibration flight segments had calculated use rates that were < 1%. As described below, these low use rates resulted in > 94% treatment efficacy. These calibrations highlight the efficiency of a surveillance operation that combines effective target control, which is fundamental to an effective containment strategy and further contributes to a limited knowledge base relating control effort to weed density (Buddenhagen and Yañez 2005; Cacho et al. 2007, Campbell et al 1996; Hester 2010; Panetta 2009; Panetta and Lawes 2005).

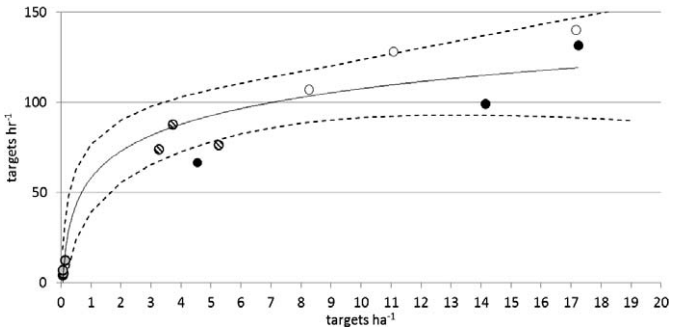

Figure 3. A scatter plot with best fit line (R^2 = 0.924; P < 0.001) with 95% confidence interval (dash lines) of target acquisition rate (targets hr^{-1}) versus target density (targets ha^{-1}) for experimental HBT helicopter operations (n = 13) conducted in Wailua nui (black), Waiokamilo 1 (white), Waiokamilo 2 (stripe) and Opaekaa (grey) from November 2010 to October 2011. See Table 4 for regression coefficients.

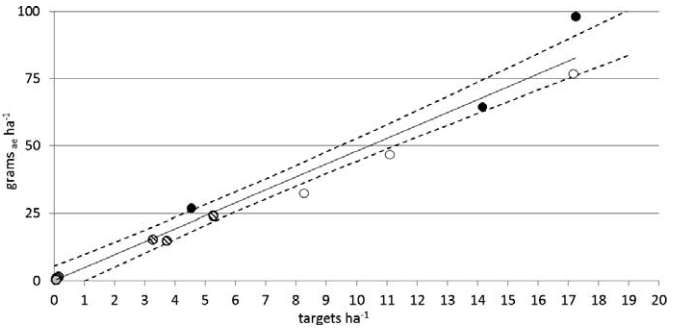

Figure 4. A scatter plot with best fit line (R^2 = 0.966; P < 0.001) with 95% confidence interval (dash lines) of herbicide acid equivalent amount (grams ae ha^{-1}) versus target density (targets ha^{-1}) for experimental HBT helicopter operations (n = 13) conducted in Wailua nui (black), Waiokamilo 1 (white), Waiokamilo 2 (stripe) and Opaekaa (grey) from November 2010 to October 2011. See Table 4 for regression coefficients.

Previously undetected targets were identified and treated in subsequent overlapping operations. The range of detection efficacy calculated among the sites was 0.427 to 0.708 with a mean of 0.560 (Table 5). Operational treatment efficacy was determined in repeat segments by identifying survivors of a previous application. Typical symptoms included severe defoliation and necrosis associated with the herbicide treatment, but with intact lateral branches retaining photosynthetic leaf canopy. Thus, survivorship was not likely due to a malfunction of the HBT-TCP200 projectiles, but rather a condition of the application under a simulated operational setting. Regardless, the lowest operational treatment efficacy recorded was 0.941 at Opaekaa with a mean of 0.972 for all of the segments. Mortality factors (i.e. product of detection and treatment efficacies) among the segments had a range of 0.424 to 0.667 with a mean value of 0.542 (Table 5). These calibrations suggest that detection efficacy is a more influential correlate of mortality factor, highlighting the difficulty of plant detection in these natural environments, but also validates the consistency of this herbicide application platform (e.g. 5-unit dose).

This study recognizes mortality factor (Cacho et al. 2006) as an important parameter generated from these HBT calibrations. A mean of 0.542 would suggest a need to improve miconia detection through better surveillance techniques. Panetta and Cacho (2012) suggest that a structured search effort with uniform coverage and overlap should optimize target detectability. According to Cacho et al. (2007) coverage is a product of speed, time and detectable sight distance. This study utilized three different pilots and six different spotters for conducting the calibration flight segments (n = 13). All participants had several years of experience in helicopter surveillance operations and miconia detection. The speeds observed

Table 4. Regression coefficients as performance analytics for search efficiency, target acquisition rate and herbicide dose from empirical calibrations (n = 13) and cost components for simulated 1-yr extirpation strategies of different management frequencies, all relative to target density (T ha^{-1}).

Dependent variable	Coefficients		R^2	P
	m	*b*		
Empirical[a]				
Search efficiency (min ha^{-1})	0.4183	1.1307	0.933	< 0.001
Target acquisition rate (targets hr^{-1})	21.533*ln	57.885	0.927	< 0.001
Herbicide dose (g ae t^{-1})	4.7937	0	0.966	< 0.001
Simulation[b]				
Qrt; MF 0.96 ($USD)	23.81	39,111	0.996	< 0.001
Semi; MF 0.79 ($USD)	20.39	19,468	0.994	< 0.001
Annu; MF 0.54 ($USD)	13.40	9,811	0.987	< 0.001

[a] Refer to Figures 2, 3 and 4 for search efficiency, target acquisition rate and herbicide dose, respectively.

[b] Refer to Figure 5 for simulations.

for these flight segments could be described as a slow hover within a ''comfort'' zone for efficient target detection, which was estimated at 5.3 km hr^{-1} (see y-intercept for search efficiency in Table 4). Speed reduction might improve target detection but with an added expense and the possibility of increasing pilot fatigue.

Miconia detectability is impeded by heavy vegetation and extreme topography, which are typical of tropical wet forest ecosystems. Plant size was also a factor in detectability. A majority of the acquired plant targets were at least 1 m tall, indicating a minimum age of 2 yr, while a majority of the incipient populations may consist of undetectable 1-yr juveniles. This highlights two points: (1) miconia detection is likely to be less than 100% and (2) recruitment of new detectable miconia can be expected in management areas within 1 yr following initial population reduction. These two conditions warrant a commitment to frequent, repeated surveillance operations of a management area that extends beyond reaching an undetectable level, if the ultimate goal is to actually achieve complete eradication of the incipient population. Ideally, this would occur under a policy that minimizes expected costs based on knowledge of the target species' biology and performance of the operational strategy (Burnett et al. 2007).

Operational costs were projected for simulated 1-yr population reduction strategies with different surveillance frequencies and plant target densities (Figure 5; Table 4). Costs for all strategies exhibited significant positive linear trends to plant target density (Table 4; $R^2 = 0.987–0.996$, $P_{0.05} < 0.001$) with semi- and quarter-annual strategies costing two- and four-fold higher than the annual strategy, respectively, where no targets were present. However, treatment costs (i.e. slope) progressively increased from lowest to highest frequency. With the cost of the herbicide

Table 5. Empirical Estimates for Detection Efficacy[a] (DE) and Operational Treatment Efficacy[b] (OTE) to calculate Mortality Factors (MF) from overlapping areas with repeated calibrations.

	Wailua Nui (7.8 ha)			Waiokamilo 1 (7.3 ha)		Waiokamilo 2 (5.7 ha)		Opaekaa (121.4 ha)	
Segments	1	2	3	1	2–3[c]	1	2–3[c]	1–3[c]	4
Targets	134	110	65	140	188	33	35	17	7
Survivors	—	4	5	—	1	—	0	—	1
DE	—	0.549	0.629	—	0.427	—	0.485	—	0.708
OTE	—	0.970	0.955	—	0.993	—	1.000	—	0.941
MF	—	0.533	0.600	—	0.424	—	0.485	—	0.667

[a] DE is calculated as the ratio of the previous targets from the total combined targets with the subsequent operation and it is assumed that all new targets in the subsequent operation were previously undetected and not new recruits.

[b] OTE is the ratio of effectively treated targets from the total targets, which is derived from the number of confirmed survivors identified in the subsequent operation.

[c] Combined calibrations overlapping the entirety of the of the previous/subsequent calibration and were conducted within 1 week of each other with targets and survivors reported as a composite value.

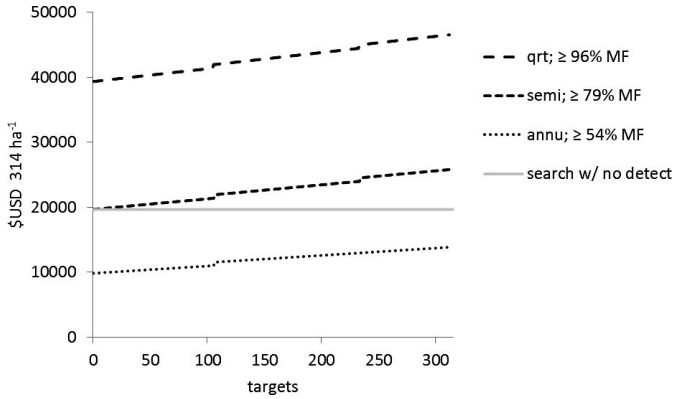

Figure 5. Expected operational cost projections of simulated 1-yr extirpation strategies within a 314-ha buffer management area with incipient population densities up to 1 target ha^{-1}. Each operation is assigned an MF = 0.542 with different management frequencies: Qrt (4 ops; MF = 0.96), Semi (2 ops, 0.79) and Annu (1 operation; MF = 0.54). Calculations based on single-helicopter operations. The solid line represents a semi-annual helicopter surveillance strategy with two operations where no targets are detected to confirm extirpation. See Table 4 for regression coefficients.

dose remaining static at $7.75 per plant, the cost increases corresponded to the extra flight time for overlapping coverage of the same area, regardless of whether the target was undetected in a prior operation or with treatment confirmation in the subsequent operation. The increases in population reduction potential (i.e. mortality factor) for the more frequent strategies is less than the corresponding cost increases, which reflects the difficulties of treating the last remaining targets to achieve undetectable levels and corroborates with Burnett et al. (2007) suggestion to defer management at extremely low target densities. The cost to search a 314-ha management area with no targets detected, along with an added surveillance operation to confirm no targets was estimated to be $19,657 USD, and served as a reference to opportunity cost for the other management options (Figure 5). For instance, this cost is comparable to a single surveillance operation of the same size management area, but with the opportunity to treat up to 734 targets at a mortality factor of 0.54, while conversely the higher frequency strategies lose opportunities to confirm undetectable levels in other management areas.

The matrix model simulated these same strategies, and included bi- and triennial schedules over a multi-yr period until complete eradication was achieved by exhausting predetermined seed banks, (Table 6). For all simulations, NPVs decreased proportionally to operational frequency and were largely influenced by the total number of operations and the discount rate applied each year across the timeline. The quarter-annual strategy achieved eradication with the shortest timelines, but also with the highest number of operations and at the least discounted rates, thus, resulting in the highest NPVs. The triennial strategy eradicated the smallest population with the lowest NPV, resulting from the longest timeline with the most discounted rates. However, this strategy failed to eradicate the two larger vector populations with reduction being outpaced by recruitment. The biennial strategy eradicated these larger vector populations, with the longest timelines and most discounted rates resulting again in the lowest NPVs. This illustrates the value of maximizing discounted rates with long-term extensions to strategies. However, this could only be accounted for with a reliable commitment to sustained resources and if those resources were actually invested on years where management was not scheduled. Miconia management programs in Hawaii operate under no such mandate and experience fiscal fluctuations with annual renewals.

These short- and long-term projections (Figure 5; Tables 4 and 6) are deterministic by producing expected outcomes, which can vary from actual results, but should continue to improve with updates in quantitative ecology and operations research (Hester et al. 2010). Cost estimates and NPVs reported in this study are within range of reported projections from Australia (Hester et al. 2010). These expected cost and NPV projections assume complete surveillance of a 314-ha isotropic buffer, but is likely to be an impractical management unit in heterogeneous environments (Murphy et al. 2008). Spatial analyses of population distribution and suitable habitat will become valuable contributions in management area prioritization and resource allocation. For example, ravines and gullies are known to serve as conduits in frugivorous dispersal and gravitational migration of propagules (Metcalf et al. 1998; Murphy et al. 2008). New information from Tahiti has identified several parameters, including topgraphic slope and aspect, as identifiers of suitable habitat for miconia (Pouteau et al 2011). The projections from this study are likely to over-estimate resource requirements to accomplish population reduction goals, although the performance of the HBT platform should be consistent regardless of management area designation. Future operational use patterns of the platform are expected to improve the calibrations with larger data sets generated by multiple applicators and a broader range of scenarios. The protocols adopted in this study for recording basic operational parameters and calibrating performance should be universal to most weed management techniques in natural areas where search effort and treatment efficacy are both critical features to successful operations (Cacho et al 2007). The HBT platform is presented as a complement to existing ground and aerial efforts for miconia management in Hawaii. Accurate calibrations of these conventional techniques will further support decisions for future assignments where HBT might be best suited.

Table 6. Projected long-term management strategies to eradicate incipient miconia populations within a 314 ha isotropic buffer management area with an operational mortality factor (MF) = 0.542.

X_t[a] (adult/jv)	Schedule[b]	Years/ops[c]	Adult/jv[d]	Mean MF[e]	NPV[f] ($1000×)
2/48	Qrt	13/38	2/264	0.977	272.87
	Semi	13/23	2/277	0.819	158.90
	Annu	13/13	3/329	0.565	87.46
	Bi	19/10	17/455	0.325	58.48
	Tri	58/20	123/1,736	0.225	57.17
20/74	Qrt	15/46	20/543	0.971	317.12
	Semi	15/27	24/628	0.809	180.22
	Annu	16/16	34/856	0.556	102.69
	Bi	29/15	110/1,653	0.306	72.99
	Tri	—	—	—	—
209/1518	Qrt	21/69	218/8,887	0.961	526.56
	Semi	21/38	281/10,111	0.782	319.58
	Annu	25/25	550/13,587	0.542	213.49
	Bi	63/32	1,491/23,050	0.405	164.79
	Tri	—	—	—	—

[a] Initial vector population of adults and detectable juveniles (yr 2 to 4).

[b] Operation frequency: Qrt - four operations yr^{-1}; Semi- two operations yr^{-1}; Annu- one operation yr^{-1}; Bi- one operation two yrs^{-1}; Tri- one operation three yrs^{-1}.

[c] Total yr and operations projected to achieve incipient population extirpation.

[d] Total adults and juvenile (yr 2 to 4) targets acquired to achieve incipient population extirpation.

[e] Mean annual mortality factor based on an operational mortality factor of 0.542 compounded by the number of operations.

[f] Net present value investment ($USD) based on cost of helicopter operations (see Table 2), projectile inventory consumption and annual discount rate of 6%.

A comprehensive miconia management strategy is limited by available fiscal resources, which force decisions to be made between risk aversion and budget optimization (Burnett et al. 2007; Hester et al. 2010). An optimal policy for miconia management minimizes the present values of management costs and residual damages along an infinite timeline, that would even dictate management deferment for low-density populations, where the marginal cost to search and treat these remaining individuals is extremely high (Burnett et al. 2007). Murphy et al. (2008) recommended the establishment of management units with a minimum 1000 m radial buffer, but in the same report identified 95% of the targets treated within a 500 m buffer. According to Burnett et al. (2007) and in this study (see Figure 5) elimination of that last 5% becomes exceedingly more difficult and costly. This study suggests a triennial schedule as an optimum strategy for the smallest incipient population, although it must accommodate a 58-yr timeline with an 8-fold recruitment of the mature population. Anecdotally, we have encountered multiple occasions confirming the establishment of mature stands when reentry to a site exceeds 2 yr. From a practitioner's standpoint, a budget optimization approach is likely to be viewed as too risky, particularly when funding provisions fluctuate annually with no permanent mandate of support.

For invasive weed management, marginal costs can be interpreted different ways, with incremental units based on target numbers or net treated area (Buddenhagen and Yañez 2005; Campbell et al. 1996; Rejmánek and Pitcairn 2002). Resources dedicated to control inputs may be negligible compared to resources dedicated to search effort (Hester et al. 2010). Helicopter flight time was a dominant cost component for analyzing HBT platform performance. We identified surveillance operations confirming undetectable levels (i.e. no targets detected) to have the lowest marginal cost that could be applied to a management area. Delimiting incipient populations is critical to effective containment of miconia, and should include expanding surveys into unknown areas despite the probability of not detecting new populations (Brooks et al. 2009; Cacho et al. 2010) However, the strategy must acknowledge the conundrum of an opportunity lost in reducing (i.e. target treatment) known, incipient populations.

This study does not attempt to provide concrete decisions in favor of extreme risk aversion or expected cost minimization. However, miconia is an autogamous species with rapid maturity, high fecundity and a large dispersal

range making a single plant in a remote area a high value target that can only be detected with resources dedicated to frequent, overlapping surveillance operations. The best utility identified so far for the HBT platform is through integration into aerial surveillance operations where nominal herbicide use rates translate into significant flight time cost savings and provides streamlined efforts towards effective miconia containment.

Acknowledgments

Funding for this project was provided in part by the Maui County Office of Economic Development Special Grants Program, Hawaii Invasive Species Council Technology Grants Program, USDA-CSREES Tropical Subtropical Agriculture Research Program, USDA-NIFA Rural Resources Extension Act, and the USDA- NRCS Conservation Innovation Grant. We thank Nelson Paint Company, Dow Agrosciences LLC., BASF Corp. and The Wilbur Ellis Company for their current and past collaborations. We thank Keren Gundersen, Lloyd Loope, Chuck Chimera and two anonymous reviewers for improving this manuscript with thoughtful suggestions.

Literature Cited

Brooks, S. J., F. D. Panetta, and T. A. Sydes. 2009. Progress towards the eradication of three melastome shrub species from northern Australian rainforests. Plant Protect. Quart. 24(2):71–78.

Buddenhagen, C. and P. Yañez. 2005. The costs of Quinine *Cinchona pubescens* control on Santa Cruz Island, Galapagos, Galapagos Res. 63:32–36.

Burnett, K., B. Kaiser, and J. Roumasset. 2007. Economic Lessons from Control Efforts for an Invasive Species: *Miconia calvescens* in Hawaii, J. For. Econ. 13(2–3):151–167.

Cacho, O. J., S. Hester, and D. Spring. 2007. Applying search theory to determine the feasibility of eradicating an invasive population in natural environments. Aus. J. Agric. and Res. Econ. 51:425–433.

Cacho, O. J., D. Spring, P. Pheloung, and S. Hester. 2006. Evaluating the feasibility of eradicating an invasion. Bio. Inv. 8:903–917.

Cacho, O. J., D. Spring, S. Hester, and N. MacNally. 2010. Allocating surveillance effort in the management of invasive species: a spatially-explicit model. Environ. Modelling and Software 25:444–454.

Campbell, S. D., C. L. Setter, P. L. Jeffrey, and J. Vitelli. 1996. Controlling dense infestations of *Prosopis pallida*. Pages 231–232 *in* R.C.H. Shepherd, ed. Proc. 11th Aus. Weeds Conf.. Weed Science Society of Victoria, Frankston.

Chimera, C. G., A. C. Medeiros, L. L. Loope, and R. H. Hobdy. 2000. Status of management and control efforts for the invasive alien tree *Miconia calvescens* DC. (Melastomataceae) in Hana, East Maui. Honolulu, HI: University of Hawaii Pacific Coop. Studies Unit, Tech Rep #128. 53 p.

Denslow, J. S. 2003. Weeds in paradise: thoughts on the invasibility of tropical islands. Ann. MO Bot. Gard. 90:119–127.

Florence, J. 1993. La végétation de quelques îles de Polynésie. Planches 54–55. *in* F. Dupon, coord. ed. Atlas de la Polynésie franç aise. ORSTOM, Paris, France.

Giambelluca, T. W., R. A. Sutherland, K. Nanko, R. G. Mudd, and A. D. Ziegler. 2010. Effects of Miconia on hydrology: a first approximation. Pages 1–7 *in* L. L. Loope, J. Y. Meyer, B. D. Hardesty, and C. W. Smith, eds. Proceedings of the International Miconia Conference, Keanae, Maui, Hawaii, May 4–7, 2009. Honolulu, HI: University of Hawaii, Maui Invasive Species Committee and Pacific Coop Studies Unit, www.hear.org/conferences/miconia2009/pdfs/giambelluca.pdf. Accessed March 2012.

Hardesty, B. D., S. S. Metcalfe, and D. A. Westcott. 2011. Persistence and spread in a new landscape: dispersal ecology and genetics of Miconia invasions in Australia. Acta Oecol., 37:657–665.

Hester, S. M., S. J. Brooks, O. J. Cacho, and F. D. Panetta. 2010. Applying a simulation model to the management of an infestation of *Miconia calvescens* in the wet tropics of Australia. Weed Res. 50(3):269–279.

Hulme, P. E. 2006. Beyond control: wider implications for the management of biological invasions. J. Appl. Ecol. 43:835–847.

Kueffer, C., C. C. Daehler, C. W. Torres-Santana, C. Lavergne, J.-Y. Meyer, R. Otto, and L. Silva. 2010. A global comparison of plant invasions on oceanic islands. Persp. Plant Ecol. Evol. Syst. 12: 145–161.

Lowe, S., M. Browne, S. Boudjelas, and M. De Poorter. 2000. 100 of the World's Worst Invasive Alien Species A selection from the Global Invasive Species Database. The Invasive Species Specialist Group (ISSG) a specialist group of the Species Survival Commission (SSC) of the World Conservation Union (IUCN), 12 p.

Mack, R. N., D. Simberloff, W. M. Lonsdale, H. C. Evans, M. Clout, and F. A. Bazzaz. 2000. Biotic invasions: causes, epidemiology, global consequences and control. Ecol. Appl. 10:689–710.

Medeiros, A. C., L. L. Loope, P. Conant, and S. McElvaney. 1997. Status, ecology and management of the invasive plant *Miconia calvescens* DC. (Melastomataceae) in the Hawaiian Islands. B. P. Bishop Museum Occasional Papers 48:23–36.

Medeiros, A. C., L. L. Loope, and R. W. Hobdy. 1998. Interagency efforts to combat *Miconia calvescens* on the island of Maui, Hawai'i. Pages 45–51, *in* J-Y. Meyer and C. W. Smith, eds. Proceedings of the first regional conference on Miconia control. August 26–29, 1997, Centre ORSTOM de Tahiti.

Metcalfe, D. J., P. J. Grubb, and I. M. Turner. 1998. The ecology of very small-seeded shade-tolerant trees and shrubs in lowland rain forest in Singapore. Plant Ecol. 134:131–149.

Meyer, J-Y. 1994. Mecanismes d'invasion de Miconia calvescens en Polynesie Francaise. Ph.D. thesis, l'Universite de Montpellier I1 Sciences et Techniques du Langueduc; Montpellier, France. 122 p.

Meyer, J-Y. 1996. Status of *Miconia calvescens* (Melastomataceae), a dominant invasive tree in the Society Islands (French Polynesia). Pac. Sci. 50:66–76.

Meyer, J-Y. 1998. Observations on the reproductive biology of *Miconia calvescens* DC (Melastomataceae), an alien invasive tree on the island of Tahiti (South Pacific Ocean). Biotropica. 30:609–624.

Meyer, J-Y., L. L. Loope, and A. C. Goarant. 2011. Strategy to control the invasive alien tree Miconia calvescens in Pacific islands: eradication, containment or something else? Pages 91–96 *in* C. R. Veitch, M. N. Clout, and D. R. Towns, eds. 2011. Island Invasives: Eradication and Management. Gland, Switzerland: IUCN.

Moody, M. E. and R. N. Mack. 1988. Controlling the spread of plant invasions: the importance of nascent foci. J. Appl. Ecol. 25: 1009–1021.

Murphy, H. T., B. D. Hardesty, C. S. Fletcher, D. J. Metcalfe, D. A. Westcott, and S. J. Brooks. 2008. Predicting dispersal and recruitment of *Miconia calvescens* (Melastomataceae) in Australian tropical rainforests. Biol. Inv. 10:925–936.

Myers, J. H., D. Simberloff, A. M. Kuris, and J. R. Carey. 2000. Eradication revisited: dealing with exotic species. Trends Ecol. Evol. 15:316–20.

PCSU (Pacific Cooperative Studies Unit). 2011. Standing Operating Procedure for Herbicide Ballistic Technology Operations: Ground and Aerial Herbicide Application. Safety Management Program. RCUH-PCSU SOP no. 32. 19 p.

Panetta, F. D. 2009. Weed eradication: an economic perspective. Inv. Pl. Plant Sci. Manag. 2(4):360–368.

Panetta, F. D. and O. J. Cacho. 2012. Beyond fecundity control: which weeds are most containable? J. Appl. Ecol.. doi: 10.1111/j.1365-2664.2011.02105.

Panetta, F. D. and R. Lawes. 2005. Evaluation of weed eradication programs: the delimitation of extent. Div. Distr. 11(5):435–42.

Pouteau, R., J-Y. Meyer, and B. Stoll. 2011. A SVM-based model for predicting the distribution of the invasive tree *Miconia calvescens* in tropical rainforests. Ecol. Model. 222:2631–2641.

Reaser, J. K., L. A. Meyerson, Q. Cronk, M. DePoorter, L. G. Eldrege, E. Green, M. Kairo, P. Latasi, R. N. Mack, J. Mauremootoo, D. O'Dowd, W. Orapa, S. Sastroutomo, A. Saunders, C. Shine, S. Thrainsson, and L. Vaiutu. 2007. Ecological and socioeconomic impacts of invasive alien species in island ecosystems. Environ. Conserv. 34:98–111.

Rejmánek, M. and M. J. Pitcairn. 2002. When is eradication of exotic pest plants a realistic goal? Pages 249–253 *in* C. R. Vietch and M. N. Clout, eds. Turning the Tide: The Eradication of Island Invasive. Gland, Switzerland: IUCN SSC Invasive Species Specialist Group.

Taylor, C. M. and A. Hastings. 2004. Finding optimal control strategies for invasive species: a density-structured model for *Spartina alterniflora*. J. Appl. Ecol. 41:1049–1057.

Wittenberg, R. and M.J.W. Cock, eds. 2001. Invasive Alien Species: A Toolkit of Best Prevention and Management Practices. Wallingford, Oxon, UK: CAB International. 241 p.

Received April 2, 2012, and and accepted January 7, 2013.

Appendix 1. Stage matrix (H) and vector populations (X_t) adopted from Hester et al 2010.

H =	0	0	0	0	0	0	Fsa	Fla	X_t =		*2/48*	*20/74*	*209/1518*
	Pfruit	Psb	0	0	0	0	0	0		SB[a]	20.80	47.99	675.45
	0	G	0	0	0	0	0	0		jv_1	3,418	4,872	95,440
	0	0	Pjv1	0	0	0	0	0		Jv_2	37	44	1012
	0	0	0	Pjv2	0	0	0	0		Jv_3	8	11	257
	0	0	0	0	Pjv3	P6	0	0		Jv_4	3	19	249
	0	0	0	0	0	Pjv4	P7	0		sa	0	8	83
	0	0	0	0	0	0	Psa	Pla		la	2	12	126

[a] Seed bank values reported in $\times 10^6$.